

Earth's Future

RESEARCH ARTICLE

10.1029/2023EF004120

Key Points:

- Simulating how N deposition interacts with precipitation seasonality can enable us to better predict when dryland watersheds become Nsaturated
- As rainfall regimes become more intermittent and/or variable, streamflow nitrate export is likely to increase, particularly when a watershed is N-limited
- Under future climate change in drylands, prolonged droughts that are followed by more intense storms may pose a major threat to water quality

Supporting Information:

Supporting Information may be found in the online version of this article.

Correspondence to:

J. Ren and E. J. Hanan, nren@unr.edu; renjianning@gmail.com; ehanan@unr.edu

Citation:

Ren, J., Hanan, E. J., D'Odorico, P., Tague, C., Schimel, J. P., & Homyak, P. M. (2024). Dryland watersheds in flux: How nitrogen deposition and changing precipitation regimes shape nitrogen export. *Earth's Future*, 12, e2023EF004120. https://doi.org/10.1029/2023EF004120

Received 13 SEP 2023 Accepted 29 MAR 2024

Author Contributions:

Conceptualization: Jianning Ren, Erin J. Hanan, Peter M. Homyak Data curation: Jianning Ren, Erin J. Hanan, Christina Tague, Peter M. Homyak Formal analysis: Jianning Ren, Erin

Formal analysis: Jianning Ren, Erin J. Hanan, Paolo D'Odorico

© 2024 The Authors. Earth's Future published by Wiley Periodicals LLC on behalf of American Geophysical Union. This is an open access article under the terms of the Creative Commons Attribution-NonCommercial-NoDerivs License, which permits use and distribution in any medium, provided the original work is properly cited, the use is non-commercial and no modifications or adaptations are made.

Dryland Watersheds in Flux: How Nitrogen Deposition and Changing Precipitation Regimes Shape Nitrogen Export

Jianning Ren¹, Erin J. Hanan¹, Paolo D'Odorico², Christina Tague³, Joshua P. Schimel⁴, and Peter M. Homyak⁵

¹Department of Natural Resources and Environmental Science, University of Nevada, Reno, NV, USA, ²Department of Environmental Science, Policy, & Management, University of California, Berkeley, CA, USA, ³Bren School of Environmental Science & Management, University of California, Santa Barbara, CA, USA, ⁴Department of Ecology, Evolution and Marine Biology, University of California, Santa Barbara, CA, USA, ⁵Department of Environmental Sciences, University of California, Riverside, CA, USA

Abstract Atmospheric nitrogen (N) deposition and climate change are transforming the way N moves through dryland watersheds. For example, N deposition is increasing N export to streams, which may be exacerbated by changes in the magnitude, timing, and intensity of precipitation (i.e., the precipitation regime). While deposition can control the amount of N entering a watershed, the precipitation regime influences rates of internal cycling; when and where soil N, plant roots, and microbes are hydrologically coupled via diffusion; how quickly plants and microbes assimilate N; and rates of denitrification, runoff, and leaching. We used the ecohydrological model RHESSys to investigate (a) how N dynamics differ between N-limited and N-saturated conditions in a dryland watershed, and (b) how total precipitation and its intra-annual intermittency (i.e., the time between storms in a year), interannual intermittency (i.e., the duration of dry months across multiple years), and interannual variability (i.e., variance in the amount of precipitation among years) modify N dynamics and export. Streamflow nitrate (NO₃⁻) export was more sensitive to increasing rainfall intermittency (both intraannual and interannual) and variability in N-limited than in N-saturated model scenarios, particularly when total precipitation was lower—the opposite was true for denitrification which is more sensitive in N-saturated than Nlimited scenarios. N export and denitrification increased or decreased more with increasing interannual intermittency than with other changes in precipitation amount. This suggests that under future climate change, prolonged droughts that are followed by more intense storms may pose a major threat to water quality in dryland watersheds.

Plain Language Summary Fossil fuel combustion and industrial agriculture have increased atmospheric nitrogen (N) pollution. Atmospheric N can travel with prevailing winds and be deposited on soil surfaces in terrestrial ecosystems. This can in turn increase N cycling and export to aquatic ecosystems, where excess N acts as a pollutant. The timing and amount of rainfall can influence how much N is transported from terrestrial to aquatic ecosystems, but it remains unclear how future N deposition and precipitation patterns will interact to influence stream water quality and drinking water security. To address this, we used a simulation model to investigate (a) how changes in the timing and/or amount of precipitation influence N export from watersheds, and (b) how the effects of precipitation change with increased atmospheric N deposition. We found that N export to streams increases with precipitation intermittency and variability, particularly when N deposition is low. Under high N deposition, export to streams is substantially elevated, regardless of precipitation timing. Our findings suggest that under future climate change, prolonged droughts that are followed by more intense storms may increase hydrologic N export and pose a major threat to water quality in dryland watersheds.

1. Introduction

Atmospheric N deposition has been increasing in dryland watersheds of the western US since the 1860s, largely due to human population growth and concomitant increases in both fossil fuel combustion and industrial agriculture (Galloway et al., 2008; Kanakidou et al., 2016). In many populated regions around the globe, N deposition is already around 20 times higher than the natural (non-anthropogenic) rate of 0.05 g N g m⁻² year⁻¹ (Dentener et al., 2006; Galloway et al., 2008). While N deposition has decreased in many places over recent decades, it remains high in many ecosystems near urban areas (Du, 2016; Du et al., 2014), and will likely further increase in

REN ET AL.

Funding acquisition: Erin J. Hanan, Joshua P. Schimel, Peter M. Homyak Investigation: Jianning Ren, Erin J. Hanan, Joshua P. Schimel, Peter M. Homyak

Methodology: Jianning Ren, Erin J. Hanan, Paolo D'Odorico,

Christina Tague

Project administration: Erin J. Hanan, Peter M. Homyak

Resources: Erin J. Hanan, Christina Tague Software: Jianning Ren, Erin J. Hanan,

Christina Tague

Supervision: Erin J. Hanan

Validation: Jianning Ren, Erin J. Hanan, Paolo D'Odorico, Christina Tague, Peter

M. Homvak

Visualization: Jianning Ren, Erin

J. Hanan

Writing - original draft: Jianning Ren,

Erin J. Hanan

Writing - review & editing: Erin

J. Hanan, Paolo D'Odorico,

Christina Tague, Joshua P. Schimel, Peter

M. Homyak

the future (Decina et al., 2020). For example, in dryland chaparral watersheds near Los Angeles, California, the N deposition rate is more than 3 g N m⁻² year ⁻¹ (Benish et al., 2022), and by 2050, rates are likely to reach 5 g N m⁻² year⁻¹ near urban areas (Bettez & Groffman, 2013; Sutton et al., 2007). Given these dramatic increases in N inputs, there is an urgent need to understand (a) the point at which dryland watersheds will no longer be able to assimilate additional N (i.e., the threshold of N deposition at which they become N-saturated) and (b) how deposited N will be transformed and exported from watersheds through both hydrologic and gaseous pathways (i. e., stream export and denitrification, respectively) under both N saturated and unsaturated conditions. Precipitation plays an important role in driving N cycling, uptake, and export (Homyak et al., 2017; Schimel, 2018). However, in drylands, these processes can act on different timescales and high precipitation variability can complicate our ability to predict the fate of atmospherically deposited N (Homyak et al., 2014; Howarth et al., 2006; Krichels et al., 2022; Ren et al., 2024a).

Conceptual models used to assess N saturation and N export were developed in temperate systems where relatively high and consistent rainfall helps maintain hydrologically connected soils, allowing substrates to diffuse to plant roots and be taken up (Homyak et al., 2014). As a result, these models assume that N export occurs once a watershed becomes N-saturated (Aber et al., 1989). In drylands, however, summer aridity can keep soils dry for months without rain, limiting diffusive N transport and allowing it to accumulate in hydrologically disconnected microsites (i.e., hotspots; Parker & Schimel, 2011). At the onset of the wet season when rains return, N can be rapidly exported before plants and soil microbes can assimilate it—this can produce large stream N losses (known as "pulses") that under traditional conceptual models would suggest N saturation (Zhu et al., 2018). However, such hydrologic losses regularly occur in drylands even when plants remain Nlimited (Homyak et al., 2014).

To better account for asynchronies between N availability and uptake, Lovett & Goodale. (2011) introduced the concept of kinetic N saturation, where available N can exceed demand over short timescales (e.g., when a storm follows a long dry period). This contrasts with capacity N-saturation, where an ecosystem or watershed can no longer assimilate N over longer timescales, resulting in consistent increases in N export that correspond with increasing atmospheric N inputs. Because both kinetic and capacity N saturation statuses can increase N export, it is difficult to identify the threshold at which dryland watersheds shift from kinetic to capacity saturation. As a result, it also remains difficult to predict the fate of atmospherically deposited N and how it changes along a gradient from kinetic to capacity saturation.

Further complicating our understanding of N saturation and export, general circulation models project changes in both the total amount and timing of precipitation in drylands (Fischer et al., 2013). These changes can occur on both intra- and interannual scales (Knapp et al., 2002; Trenberth et al., 2003). On intra-annual time scales, a higher water-holding capacity in a warming atmosphere can give rise to larger precipitation events with longer dry periods between storms (i.e., higher intra-annual intermittency, Allen & Ingram, 2002). At interannual scales, climate change can alter atmospheric circulation and moisture transport to promote extreme wet months with a longer duration of dry months across multiple years (i.e., higher interannual intermittency (Allen & Ingram, 2002; Trenberth et al., 2003)). Alternatively, some models project that climate change will enhance interannual variability, making dry years drier and wet years wetter, while still retaining the intra-annual storm event characteristics (Pörtner et al., 2022). Higher precipitation intermittency and variability can both affect N export, but increases in intermittency, which change both the timing and magnitude of storms (i.e., fewer, more intense storms), may have a different effect than changes in variability alone (which only influences storm size without changing timing (Homyak et al., 2017; Winter et al., 2023)). Recent studies have shown that enhanced precipitation variability and intermittency can increase both nitric oxide (NO) and nitrous oxide (N2O) emissions from soils and streams, as well as stream nitrate export (Krichels et al., 2022; Winter et al., 2023; Xiao et al., 2019). However, most of these studies are event-based and the longer-term effects of altered precipitation regimes and their interactions with N deposition remain poorly understood.

A simulation modeling approach should be useful for identifying the threshold of atmospheric N deposition at which a watershed transitions from kinetic to capacity saturation, which would enable us to better project future N export. With this approach, we can directly investigate how N export responds to temporal asynchrony between N availability and uptake; for example, when the first rain event of a wet season flushes N while plants are not actively growing (in a Mediterranean climate) versus when activation of the rainy season overlaps with the peak growing season in early spring (in a continental climate). We expect that when a watershed only experiences

REN ET AL. 2 of 21 kinetic saturation, there will be pronounced differences between these two scenarios because N is flushed to streams before plant uptake in the Mediterranean climate scenario. Conversely, when a watershed is capacity N-saturated due to high N-deposition, total N export will not change in response to the timing of precipitation.

We aim to understand how N saturation status, precipitation intermittency, variability, and total amount of precipitation can interact to influence N export in a dryland watershed in California. Using a simulation modeling approach, we first developed and tested our proposed metric for identifying when a dryland watershed becomes "capacity N-saturated." Then using the new metric, we developed N-limited and N-saturated scenarios to address two questions: (a) How do changes in the precipitation regime, including the total amount of precipitation, its intra-annual intermittency, interannual intermittency, and interannual variability influence watershed-scale N export, and (b) How do these responses differ between N-limited and N-saturated watersheds? These scenarios were conducted using the coupled ecohydrological-biogeochemical model RHESSys (Tague & Band, 2004) in a dryland, chaparral-dominated watershed downwind of Los Angeles, California that experiences high rates of N deposition.

2. Methods

2.1. Study Site

We developed modeling scenarios for the chaparral-dominated Bell 4 watershed in the San Dimas Experimental Forest, located 50 km northeast of Los Angeles, California (34°12′N, 117°47′W). This is a small watershed (0.14 km²) with elevations ranging from 700 to 1,024 m. The soils are shallow, coarse-textured sandy loams weathered from granitic parent material (Chaney et al., 2016; Dunn et al., 1988); they are classified as Typic or Lithic Xerorthents (Hubbert et al., 2006; Ryan, 1991a, 1991b). The climate is characterized by hot and dry summers and cool-humid winters. Mean annual precipitation is approximately 700 mm. Mean annual air temperature is 15.5°C with daily temperatures ranging from -8°C in winter to 40°C in summer. Vegetation on southfacing slopes includes chamise (*Adenostoma fasciculatum*), California lilac (*Ceanothus spp.*), and black sage (*Salvia mellifera*), while north-facing slopes are covered by *ceanothus spp.* and California laurel (*Umbellularia californica*). Riparian areas are dominated by live oak (*Quercus agrifolia*). Being downwind from a major metropolitan area, Bell 4 experiences high N deposition rates, which exceed 30 kg ha⁻¹ year⁻¹ (Benish et al., 2022; Bytnerowicz & Fenn, 1996).

2.2. RHESSys Model

To investigate how precipitation regime changes affect N cycling and export in drylands and how they are different between N-limited and N-saturated watersheds, we used the regional hydro-ecologic simulation system (RHESSys). RHESSys is a spatially distributed model that fully couples hydrological processes with biogeochemical processes, allowing it to simulate the effects of climate and environmental change on C and N cycling and hydrologic conditions (Garcia et al., 2016; Lin et al., 2015; Tague & Band, 2004). Recent model improvements have enabled RHESSys to better represent N cycling and transport in dryland watersheds (Burke et al., 2021; Hanan et al., 2017; Ren et al., 2024a) This includes refining nitrification processes after wildfire in chaparral (Hanan et al., 2017), and representing biogeochemical hotspots explicitly across a landscape (Ren et al., 2024a). RHESSys has been extensively evaluated in several dryland watersheds across the western US, for processes including N leaching (Chen et al., 2020; Hanan et al., 2017; Stephens et al., 2022); C dynamics (Burke et al., 2021; Garcia et al., 2016; Hanan et al., 2021; Ren et al., 2022; Reyes et al., 2017), and hydrologic responses to climate change and forest disturbances (Garcia & Tague, 2015; Hanan et al., 2021).

C and N cycling among vegetation, litter, and soil layers are simulated at a patch scale (the smallest spatial unit; 3-m resolution in this study). Photosynthesis is calculated using the Farquhar model which is a function of stomatal conductance, radiation, nitrogen and carbon dioxide concentration, air temperature, and atmospheric pressure (Farquhar & von Caemmerer, 1982). Plant respiration includes maintenance and growth respiration, which is estimated using Ryan (1991a, 1991b) model. Carbon is then allocated to roots, stems, and leaves using an architecture (or age) based method (Dickinson et al., 1998). RHESSys has four litter pools and four soil pools with different C:N ratios and decomposition rates. Decomposition is estimated based on a defined maximum decomposition rate and constrained by soil moisture, soil temperature, and nitrogen availability. N mineralization and immobilization are estimated using the C:N ratios of the litter and soil pools when materials decompose from one pool to another (Hanan et al., 2017; Tague & Band, 2004).

REN ET AL. 3 of 21

RHESSys calculates nitrification rates based on the CENTURY_{NGAS} model which is a function of soil pH, soil moisture, soil temperature, and available soil ammonium (Parton, 1996). A maximum denitrification rate is calculated as a function of the total available nitrate in soil, and total soil carbon and nitrogen, and then the maximum rate is modified based on soil moisture and soil respiration as a proxy for microbial abundance.

Soil moisture processes include four vertical layers, a surface detention store, a root zone store, an unsaturated store, and a saturated store. At a daily timestep, the surface detention store receives water from canopy throughfall and snowmelt (when present), and infiltrates into the soil based on the Phillip (1957) infiltration equation. Overland flow is generated when the ponded water is above the detention storage capacity. Water can percolate into a deeper ground water store through bypass flow. Water drains from the unsaturated zone or root zone to the saturated zone based on hydraulic conductivity and moves from the saturated zone to the unsaturated zone or root zone based on the Eagleson (1978) equation. Subsurface lateral flow between patches follows topographic gradients and soil hydraulic parameters such as saturation deficit and transmissivity. Nitrate moves with these water fluxes based on its concentration (Tague & Band, 2004). Atmospherically deposited N enters the soil through infiltration from the surface detention store. In the unsaturated zone, soil nitrate decreases exponentially with depth. In the saturated zone, nitrate export follows a flushing hypothesis, where more soil nitrate becomes available for flushing to streams as the water table rises (Chen et al., 2020).

To account for sub-grid scale heterogeneity in vegetation cover, RHESSys can be run using a new aspatial framework (Burke et al., 2021). In this new framework, "patch families" are the smallest spatially explicit model unit, and "aspatial patches" nested within a patch family are the smallest aspatial model unit. Aspatial patches do not have physical locations, but instead represent a distribution of vegetation types based on observed or hypothetical distributions. Local routing of water between aspatial patches within a patch family is based on the relative moisture differences among aspatial patches in the rooting and unsaturated zones and mediated by user-defined gaining and losing coefficients for each patch type (Burke et al., 2021). Local routing in the saturated zone is based on the differences in the groundwater table and it carries nitrate when exchanging water.

We also recently expanded the aspatial patch framework to incorporate the role of fine-scale biogeochemical "hotspots," represented as aspatial patches within each patch family—these represent a distribution of microsites (e.g., soil aggregates) where biogeochemical cycling can be hydrologically disconnected, as soils dry out, from other aspatial patches that contain plant roots (Ren et al., 2024a). Hotspots help drive kinetic N saturation by enabling N to accumulate and subsequently be flushed from the system when soils are rewetted. To model hotspot dynamics, the framework includes: (a) model algorithms that enable hotspots to access soil and litter C and N from neighboring non-hotspot patches for decomposition and biogeochemical cycling, and (b) algorithms and parameters that control the moisture conditions under which hotspots are hydrologically disconnected from other aspatial patches in the saturated zone, (c) parameters that control water diffusion in the unsaturated and/or root zone between hotspot and non-hotspot patches as soils dry out. For detailed descriptions of the RHESSys model and the new hotspot framework, refer to Tague and Band (2004) and Ren et al. (2024a).

2.3. Data

To represent topography across the watershed, we used a 1-m resolution digital elevation model (DEM) from LiDAR aggregated to 10-m (Ren et al., 2024a). Soil texture was delineated across the watershed using the POLARIS database (Chaney et al., 2016). To map landcover across Bell 4, we aggregated 1-m resolution land cover data from the National Agriculture Imagery Program (NAIP; collected on 5 June 2016) to 3-m. We then classified three land cover types across the watershed: chaparral, live oak, and bare ground (Maxwell et al., 2017). RHESSys patch families were established based on the 10-m DEM, while the aspatial patch vegetation distributions were classified based on the 3-m NAIP data (Ren et al., 2024a). The Bell 4 basin contained 1,259 patch families, with each patch family having approximately 11 aspatial patches. We acquired meteorological forcing data from 1979 to 2020 from the gridMET, including daily maximum and minimum temperatures, precipitation, relative humidity, radiation, and wind speed (Abatzoglou, 2013). Daily streamflow data from 1980 to 2002 and streamflow nitrate data from 1988 to 2000 were provided by U.S. Forest Service (USFS).

2.4. Model Initialization and Calibration

To establish the soil C and N pools at a steady state, we spun RHESSys up for around three hundred years starting with quasi-equilibrium state values. Then to initialize vegetation C and N pools, we used a target-driven spin-up

REN ET AL. 4 of 21

approach, which leverages remotely sensed LAI calculated from NAIP (at 24 April 2010) to set target values for each patch across the watershed; this enables us to spin the model up mechanistically while still capturing landscape heterogeneity (Hanan et al., 2018). We then calibrated six soil parameters using observed streamflow data: saturated hydraulic conductivity ($K_{\rm sat}$), the decay of $K_{\rm sat}$ with depth (m), pore size index (b), air entry pressure (ϕ), bypass flow to deeper groundwater storage ($g_{\rm w}_1$), and deep groundwater drainage rates to stream ($g_{\rm w}_2$). We selected the best parameters by comparing the observed and modeled streamflow using the monthly Nash-Sutcliffe efficiency (NSE; Nash & Sutcliffe, 1970) and percent error of annual streamflow. We used 8 years of streamflow data from 1993 to 2002 for calibration and 3 years from 1980 to 1983 for validation. Following calibration, we designated one aspatial patch in each patch family to represent hotspots, assuming that hotspots were evenly distributed across the landscape. We then optimized the hotspot-related parameters (i.e., the water sharing coefficient between aspatial patches and subsurface flow threshold) by comparing modeled and observed streamflow nitrate from 1988 to 2000. A more detailed description of initialization and calibration results can be found in Texts S1–S3 and Figures S1–S2 in Supporting Information S1.

2.5. Scenarios

2.5.1. Developing Better Metrics for N-Saturation in Dryland Watersheds

Conventional methods that focus on streamflow N as an indicator of capacity N saturation often fail in dryland watersheds where seasonal N export occurs even when watersheds are N-limited (i.e., due to kinetic saturation; Homyak et al., 2014). Thus, we need a better metric for identifying when a watershed shifts from kinetic to capacity N saturation (Lovett & Goodale, 2011). This requires understanding how N deposition interacts with the timing of precipitation. To determine the N deposition threshold at which a watershed becomes N-saturated, we built scenarios considering interactions between the N deposition rate and precipitation seasonality over a period of 60 years. Because the observed meteorological forcing data spans only 40 years (water years 1980–2020), we repeated this data to construct the additional 20 years. This included three scenarios for precipitation seasonality: a dry summer scenario (to match observations), a wet summer scenario (to represent a more continental climate), and an evenly distributed scenario (Figure 1a). The wet summer and evenly distributed scenarios were reconstructed from the observed precipitation data by manipulating the duration of dry days and the timing of precipitation using a method from Rodriguez-Iturbe et al. (1999) which will be introduced in detail in Section 2.5.2. We also included 12 dry N deposition scenarios (including 0.05, 0.25, and 0.5-5 g m⁻² year⁻¹ at an increment of 0.5 g m⁻² year⁻¹). This range assumes that N deposition rate of 0.05 g m⁻² year⁻¹ is the natural rate which indicates a N-limited system, and 5 g m⁻² year⁻¹ makes the system heavily polluted (Dentener et al., 2006; Galloway et al., 2008). This resulted in 36 scenarios for precipitation and N deposition in a factorial design.

To determine the level of N deposition at which our watershed becomes N-saturated, we examined N export for each scenario and determined the magnitude of N deposition where export no longer varied under different precipitation seasonality scenarios. This approach assumes that under kinetic saturation, dry summers would promote more N export because rainfall occurs when plants are less active. We define the N deposition threshold above which the watershed is capacity N saturated as the amount of N deposition required for mean normalized streamflow N (i.e., annual streamflow N divided by the N deposition rate) in both the dry summer and the evenly distributed scenarios to be above 90% of the mean normalized streamflow in the dry winter scenario. Using this threshold, we then built two scenarios for N saturation status: N-saturated and N-limited. This involved scaling N deposition up or down such that the N saturated scenario had 100 times higher N deposition than the N-limited scenario. We then used these scenarios for the sensitivity analysis of the following sections to examine how precipitation intermittency and variability influence N export under saturated and unsaturated conditions. In our study, our primary focus is on dry atmospheric N deposition, and in the following sections any mention of N deposition specifically pertains to dry N deposition.

2.5.2. Effects of Intra-Annual Precipitation Intermittency on N Export

To understand how intra-annual precipitation intermittency influences N export, we used a stochastic precipitation generator, based on Rodriguez-Iturbe et al. (1999). Within a given year, the occurrence and amount of total daily precipitation can be viewed as a stochastic process. Specifically, the occurrence of rainfall is modeled as a *Poisson process with a rate* λ (average rainfall frequency), and the amount of rainfall for each event is determined

REN ET AL. 5 of 21

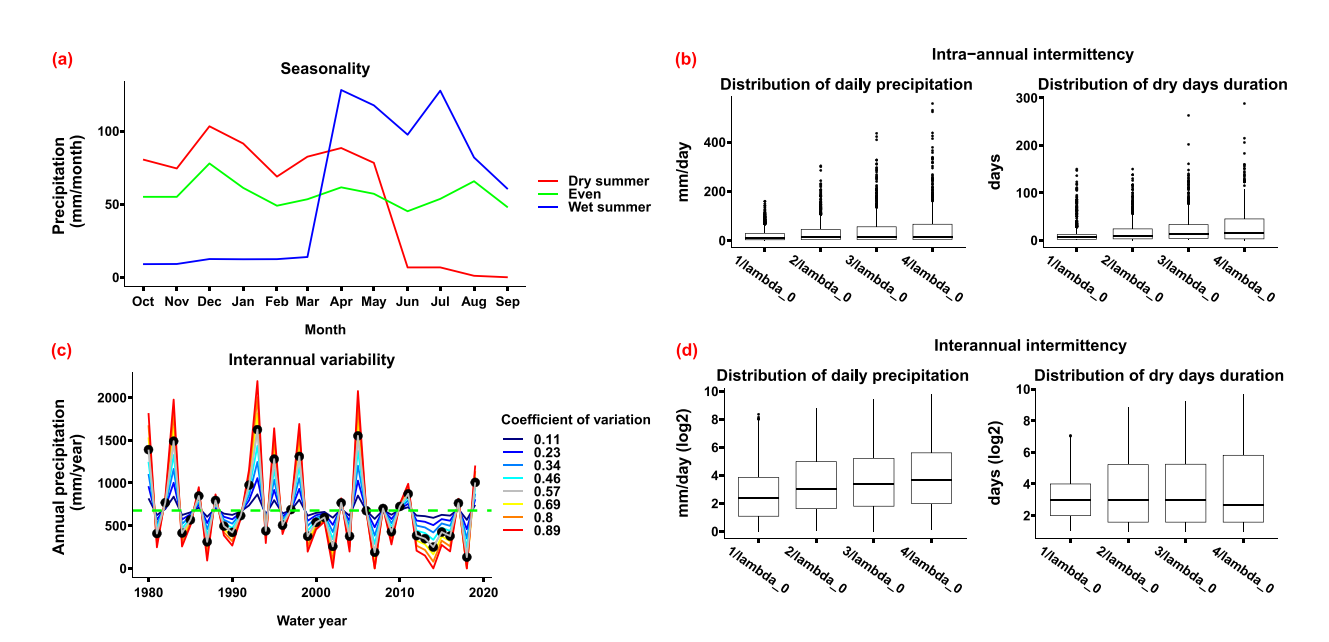


Figure 1. A summary of reconstructed precipitation data used. Panel (a) represents the precipitation seasonality scenarios: dry summer, evenly distributed across the year, and wet summer. The dry summer scenarios used observed precipitation data. Total precipitation and inter-annual intermittency over the 40 years were consistent across three scenarios. Panel (b) represents the reconstructed precipitation data with different intra-annual intermittencies for a period of 40 years, including the distribution of daily precipitation and dry days duration. The total amount of precipitation over 40 years was the same for all four precipitation intermittency scenarios. Lambda (λ_0) is the frequency of observed rain events, and the *x*-axis shows an increase in intermittency. The comparison between observed and reconstructed precipitation of $1/\lambda_0$ is shown in Figure S3 in Supporting Information S1. Panel (c) represents reconstructed and observed precipitation for different levels of interannual variability. The green horizontal line is the mean annual precipitation from the observation data and the black dots are the observed annual precipitation. Blue lines correspond with lower variability relative to observation, red lines correspond with higher variability relative to observation. Panel d represents reconstructed precipitation data with different interannual intermittencies for a period of 40 years, including the distribution of daily precipitation amounts and the distribution of duration of dry days. The total amount of precipitation over 40 years was the same for all five precipitation scenarios at a given precipitation scaling factor. Lambda (λ_0) is the frequency of reconstructed baseline rain events, and the *x*-axis shows an increase in intermittency. Note that the *y* axis is in \log_2 scale to better show extreme values.

by a random exponential distribution. As our model operates on a daily timestep, we did not consider the temporal structure of rainfall within each event and instead assumed the precipitation occurred instantaneously.

Based on these assumptions, the distribution of the length of dry days (τ) between precipitation events is an exponential distribution with a mean $1/\lambda$ (the unit of λ is 1/day).

$$f_{\tau}(\tau) = \lambda e^{-\lambda \tau}, \text{for } \tau \ge 0$$
 (1)

23284277, 2024. 4, Downloaded from https://agupubs.onlinelibrary.wiley.com/doi/10.1029/2023EF004120 by University Of California, Wiley Online Library on [14/07/2024]. See the Terms and Conditions (https://onlinelibrary.

The amount of precipitation is an independent random variable h (mm/day), calculated by an exponential probability density function:

$$f_H(h) = \frac{1}{\alpha} e^{-\frac{h}{\alpha}} for \ h \ge 0 \tag{2}$$

Where α is the mean of daily rainfall amount (mm/day) when precipitation occurs for a certain year and can be estimated from the observed data.

The total amount of precipitation R (mm year⁻¹) for a given year can therefore be calculated as

$$R = h \times T/\tau \tag{3}$$

Where *T* is the total days for a rainy season.

We estimated the two parameters (λ_0 and α) for the stochastic model based on observed precipitation. Then we adjusted the rainfall frequency parameter $1/\lambda_0$ by a factor of 2–4 to increase the duration of dry days between

REN ET AL. 6 of 21

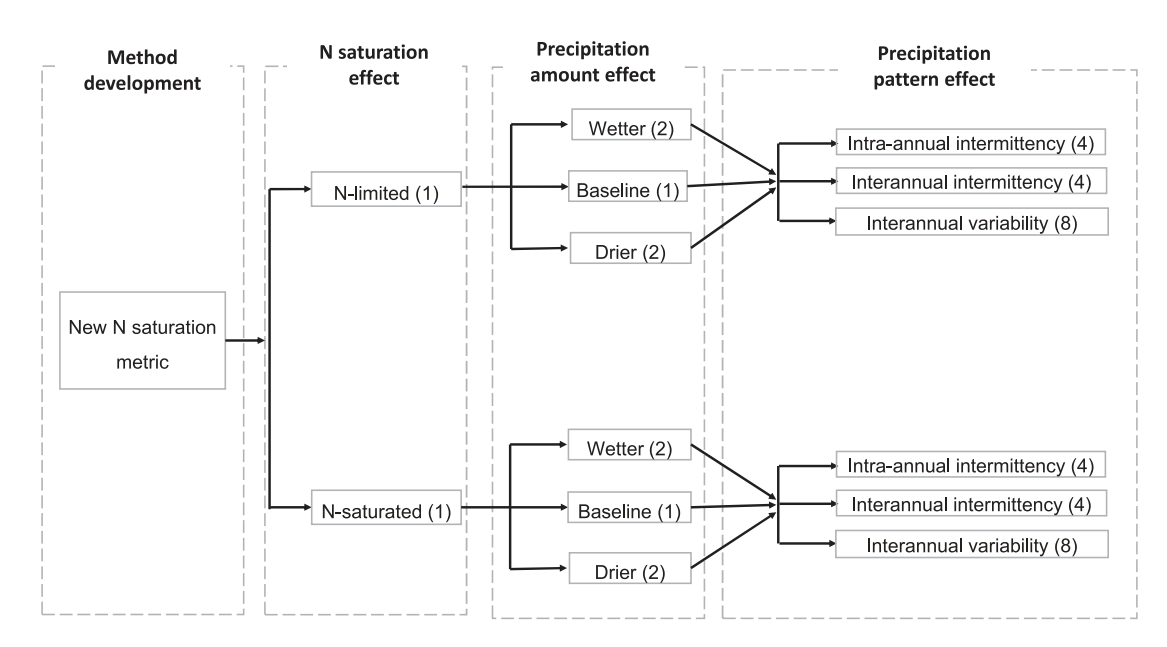


Figure 2. Summary of the scenarios developed to examine how interactions between N deposition and changes in precipitation regime affect N export. The number inside the parenthesis indicates the number of corresponding scenarios.

rainfall events. Additionally, we adjusted the mean daily rainfall amount α to maintain consistent total precipitation amounts across different scenarios. In total, we developed four distinct intra-annual intermittency scenarios (Figure 1b).

To summarize, within 1 year, this method determines the number of dry days across a rainy season and uses rainfall intensity and the number of days with precipitation (from observations) to determine the size and timing of storms that occur between dry days. This enables us to vary rainfall intermittency, while maintaining a fixed amount of precipitation for each year. Then, to examine how precipitation intermittency interacts with the total amount of precipitation (e.g., under drier vs. wetter futures), we developed five precipitation scalers for each intermittency scenario (ranging from 0.6 to 1.4 at an increment of 0.2). Hereafter, we refer to scenarios with precipitation scaling factors less than one as "drier future" scenarios and greater than one as "wetter future" scenarios. By combining five precipitation scaling factor scenarios, two N saturation scenarios, and four intraannual intermittency scenarios, we generated a total of 40 different scenarios in a factorial design and ran the model for 60 years (Figure 2).

2.5.3. The Effect of Interannual Intermittency on N Export

To investigate the effects of interannual precipitation intermittency on N export, we used a stochastic precipitation generator that was similar to the one used for the intra-annual precipitation intermittency analysis. Specifically, we examined monthly precipitation data for a period of 40 years (in total 480 months) and modeled both the amount of monthly precipitation and duration of dry months as stochastic processes. We initially ignored the temporal structure of precipitation within each month and calculated the two parameters $\lambda_{-}0$ (unit is 1/month) and α (mm/month). We first calculated a scaling factor by dividing modeled monthly precipitation by observed precipitation. We then downscaled the monthly precipitation to a daily timestep by multiplying each observed rainfall event by the scaling factor to preserve the temporal structure of rainfall events within a month. To increase the interannual intermittency, we then manipulated the two parameters (λ and α) to increase both the duration and the mean amount of monthly precipitation while maintaining consistent total precipitation levels over the 40-year period (Figure 1d). Again, we built 40 scenarios by combining the four interannual intermittency scenarios with the previous five precipitation scaling factors and the two N saturation scenarios and ran RHESSys for 60 years by looping the 40 years reconstructed data.

REN ET AL. 7 of 21

23284277, 2024, 4, Downloaded from https://agupubs.onlinelibrary.wiley.com/doi/10.1029/2023EF004120 by University Of California, Wiley Online Library on [1407/2024]. See the Terms

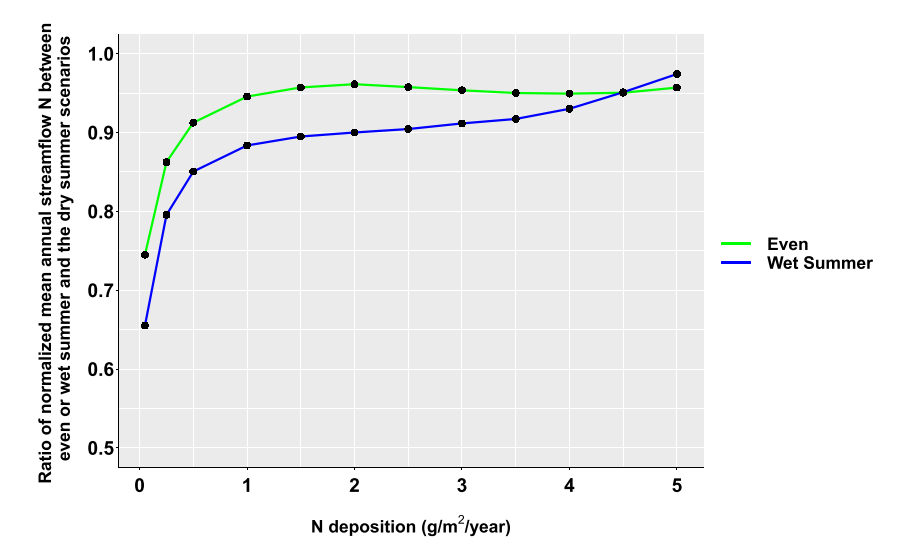


Figure 3. Ratio of the normalized mean annual streamflow nitrate export between scenarios (calculated as wet summer/dry summer (blue line) or even/dry summer (green line); values are normalized by the N deposition rate). We selected an N saturated threshold where normalized streamflow N in the wet summer scenario was no smaller than 90% of that observed in the dry summer scenario. We used mean, rather than median values to account for extreme values.

2.5.4. Effect of Interannual Precipitation Variability on N Export

To understand the effects of interannual precipitation variability on N export, we adapted methodology proposed by Gherardi and Sala (2015). We generated different scenarios for interannual precipitation variability by manipulating the observed precipitation data. To increase variability, we increased the annual precipitation amount in wet years and decreased it in dry years (by 20%, 40%, 60% relative to the observed amounts). To decrease variability, we lessened the amount of annual precipitation in wet years and increased it in dry years (by 20%, 40%, 60%, and 80%). This approach enabled us to create scenarios with varying coefficients of variation (CV) while keeping the total precipitation the same throughout the simulation period. This resulted in eight interannual variability scenarios including a baseline scenario (Figure 1c). By combining them with five total precipitation scaling factors, and two levels of N saturation (N-limited vs. N-saturated), we generated 80 factorial scenarios.

To summarize, we developed two scenarios for N saturation status (N-saturated vs. N-limited), five precipitation scaling factors (0.6, 0.8, 1, 1.2, 1.4), and three sets of scenarios for changes in precipitation timing. These changes include four intra-annual intermittency scenarios, four interannual intermittency scenarios, and eight interannual variability scenarios. This resulted in 160 factorial scenarios (Figure 2). We then calculated the normalized differences in N fluxes for each precipitation regime relative to its baseline, defined as the lowest variability or intermittency scenario for each precipitation scaling factor and N saturation status. For example, in the N-limited scenarios, to compare N export among intra-annual intermittency scenarios at a given precipitation scaling factor, we calculated differences between a given intermittency scenario and the baseline $(1/\lambda_{-}0)$. This resulted in five baseline intermittency scenarios (two drier, two wetter, and a scenario with the baseline precipitation intermittency and total amount). The combination of high precipitation scaling factors and high intermittency/variability can interact to create some extreme storms that are historically unprecedented, though within the range of possible future projections (Knapp et al., 2015). However, median storm sizes are well within the range of historical variability for these semiarid systems; we focus on median values in our discussion.

3. Results

3.1. A Better Metric for N Saturation in Drylands

In scenarios with relatively low atmospheric N deposition (i.e., smaller than 1 g m⁻² year⁻¹), the mean and distribution of annual streamflow N (over 60 years) varied depending on the seasonality of precipitation, with the dry summer scenario resulting in the highest export and the wet summer scenario resulting in the lowest (Figure 3

REN ET AL. 8 of 21

23284277, 2024, 4, Downloaded from https://agupubs.

onlinelibrary.wiley.com/doi/10.1029/2023EF004120 by University Of California, Wiley Online Library on [14/07/2024]. See

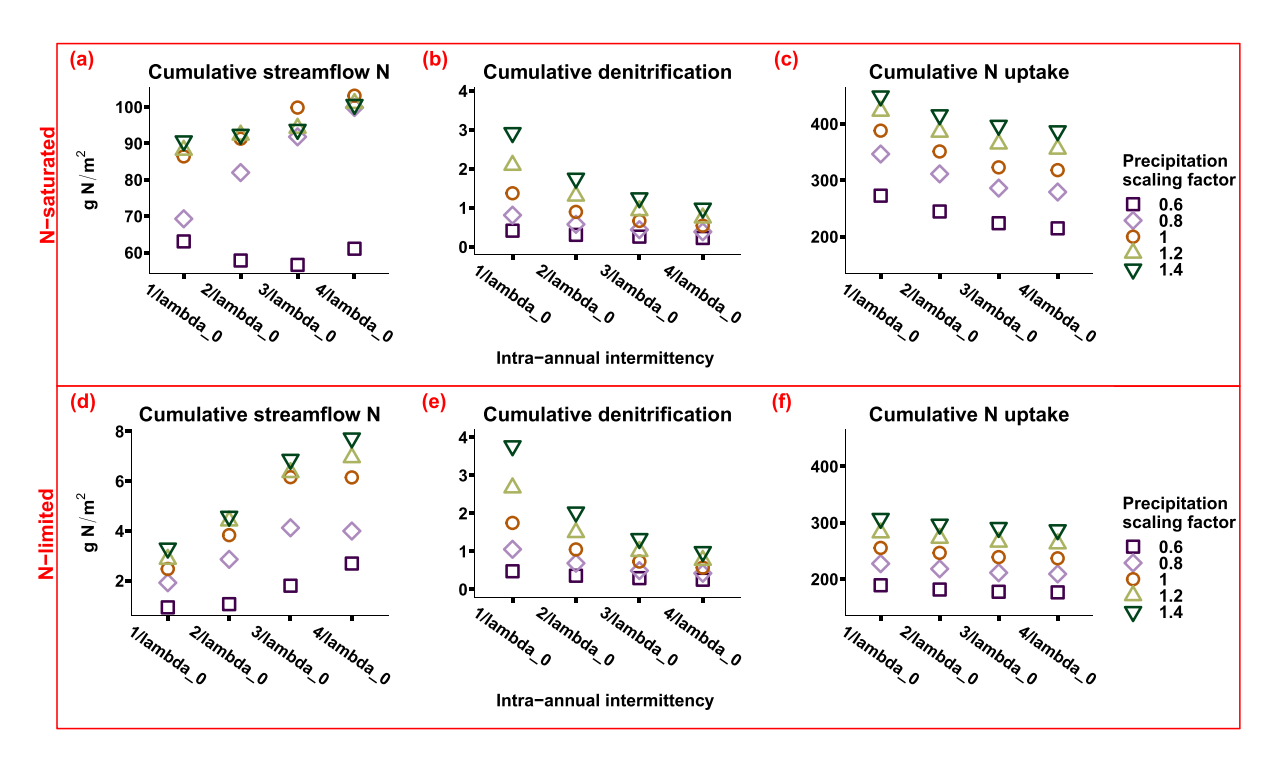


Figure 4. Sensitivity of cumulative N fluxes over 60 years (absolute value) to intra-annual precipitation intermittency for N-saturated and N-limited scenarios. The *x* axis is the duration of dry days between rainfall events, larger values represent higher intra-annual intermittencies.

and Figure S4 in Supporting Information S1). However, as N deposition increased, the watershed became less N-limited, leading to similar mean values and streamflow N distributions across different precipitation seasonality scenarios. This can be attributed to the fact that in a watershed with dry summers, the wet winter period can flush N to streams before plants begin to take it up, whereas in watersheds with wet summers, N is consumed by plants prior to leaching, resulting in less streamflow nitrate export. Consequently, it can be inferred that when the watershed is N-limited, the dry summer scenario would yield higher streamflow nitrate export than the dry winter scenario. Conversely, in an N-saturated watershed, the consumption of N by plants and microbes would have a much smaller effect on streamflow nitrate export. Using this logic, we identify an N deposition threshold of approximately 2 g m $^{-2}$ year $^{-1}$ above which the watershed becomes N-saturated. At this threshold, the ratio of the normalized mean annual streamflow N for the wet summer:dry summer scenarios was no smaller than 0.9 (the same was true for the evenly distributed scenario; Figure 3). For the following scenarios, we selected 0.05 g m $^{-2}$ year $^{-1}$ and 5 g m $^{-2}$ year $^{-1}$ to represent extremes of N-limited and N-saturated systems, respectively.

3.2. The Effect of Changing Precipitation Regimes on N Export

3.2.1. The Effect of Intra-Annual Precipitation Intermittency on N Export

Streamflow nitrate export increased with higher intra-annual intermittency, which alters both the timing and magnitude of storms (Figure 4). Moreover, in N-limited scenarios, a higher total precipitation scaling factor generally increased streamflow nitrate export (Figure 4). However, in N-saturated scenarios, baseline conditions can lead to more streamflow nitrate export (Figure 4a). Higher intermittency implies longer dry periods and greater differences in precipitation amount between dry and wet periods, despite the same total precipitation among scenarios over the 60-year simulation. This can increase soil N accumulation during dry periods while reducing denitrification and N uptake (model estimates of plant carbon declined from 6 kg m⁻² to around 4 kg m⁻² between the highest and lowest intermittency scenario, Figure S5b in Supporting Information S1). As a result, more nitrate is flushed to streams during the wet periods. For both N-limited and N-saturated scenarios, denitrification decreased with higher levels of intermittency (Figures 4b and 4e), primarily due to slower rates of decomposition caused by decreases in plant growth and litter production (Figure S5a in Supporting Information S1).

REN ET AL. 9 of 21

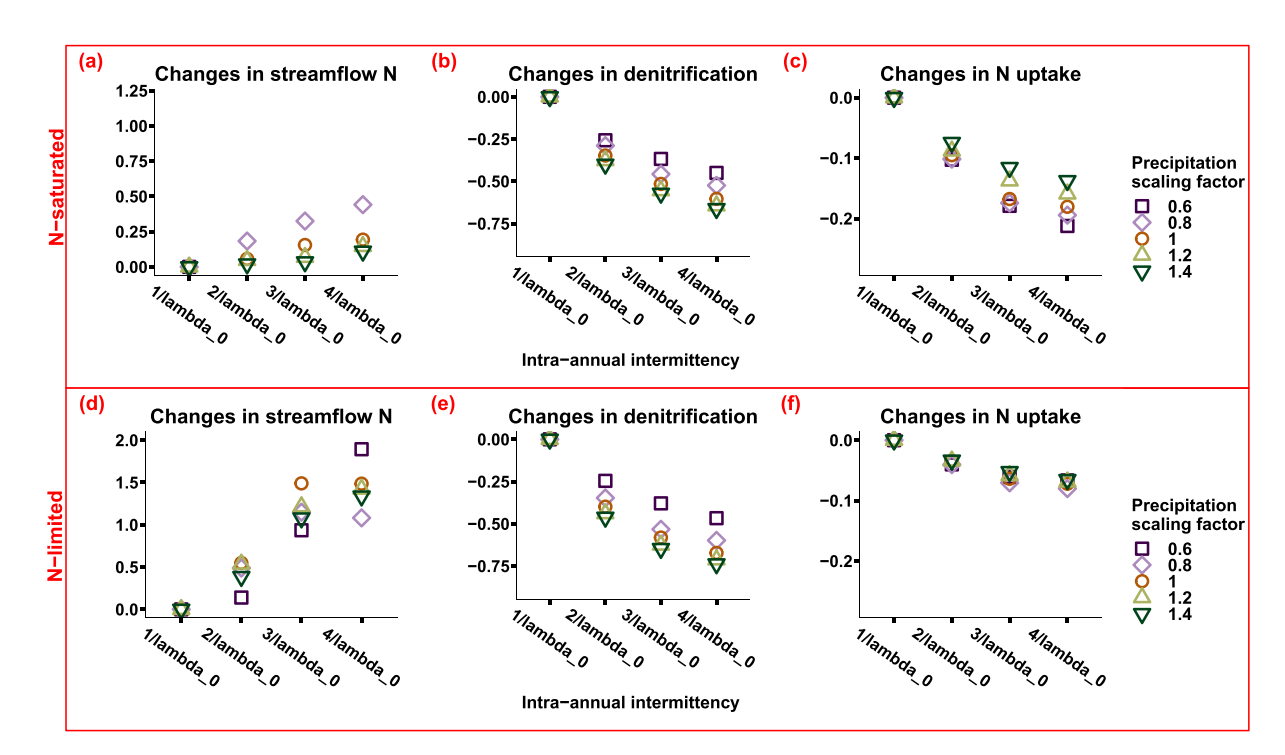


Figure 5. Sensitivity of cumulative N fluxes over 60 years to intra-annual precipitation intermittency for N-saturated and N-limited scenarios (normalized differences relative to baseline; $1/\lambda_{-}0$). The x-axis is intermittency, the y-axis is normalized change of other intermittencies relative to their baseline intermittency scenarios ($1/\lambda_{-}0$) for every precipitation scaling factor (different precipitation scaling factor scenarios have different baseline intermittency scenarios). The normalized change is calculated as $(N_{higher}-N_{baseline})/N_{baseline}$, where N_{higher} is the N flux at higher intermittency and $N_{baseline}$ is the N flux at baseline intermittency which is $(1/\lambda_{-}0)$. The top panels are N-saturated and bottom panels are N-limited scenarios.

Streamflow nitrate export and denitrification were more sensitive to intra-annual precipitation intermittency in N-limited scenarios than in N-saturated scenarios, while plant N uptake was more sensitive to intra-annual intermittency in N saturated scenarios (Figure 5). For example, plant C declined 12% (from 3.9 to 3.4 kg m $^{-2}$) in N-limited scenarios but declined 27.5% (from 5.8 to 4.2 kg m $^{-2}$) in N-saturated ones (Figure S5a in Supporting Information S1). The declines in plant carbon with higher intra-annual intermittency were smaller in N-limited scenarios because plants can be limited by both N and water, and changing water availability does not matter as much in N-limited as it does in N saturated scenarios, where once N limitation was alleviated, vegetation growth became more limited by water availability. In addition, streamflow nitrate export increased with higher levels of intra-annual intermittency, while denitrification decreased (Figures 5a and 5b). This suggests increases in intra-annual intermittency can increase nitrate export to streams while decreasing N losses to the atmosphere.

In N-saturated scenarios, streamflow nitrate export was most sensitive to variation in intra-annual intermittency under a precipitation scaling factor of 0.8, while in N-limited scenarios, scaling factors of 0.6 or 1 were the most sensitive (Figures 5a and 5b). In N-limited scenarios, the 0.6 scaling factor showed the strongest exponential increases in streamflow nitrate export with increasing intermittency, indicating that the drier future scenarios have the largest sensitivity to intermittency changes.

Denitrification in the wetter future scenarios decreased more with increasing intra-annual precipitation variability than in the drier future scenarios because total denitrification was higher in wetter baseline intermittency scenarios ($1/\lambda_{-}0$). With greater intra-annual intermittency, these decreases were larger (Figures 5b and 5e). By contrast, in dry scenarios, plant N uptake decreased slightly more with increasing intra-annual intermittency than in wetter scenarios, but the magnitude was relatively small compared to streamflow nitrate export and denitrification (Figures 5c and 5f).

3.2.2. The Effects of Interannual Precipitation Intermittency on N Export

Greater interannual intermittency and higher levels of precipitation increased streamflow nitrate export and this effect was consistent across both N-limited and N-saturated scenarios (Figure 6). Denitrification exhibited two

REN ET AL. 10 of 21

23284277, 2024, 4, Downloaded from https://agupubs.

onlinelibrary.wiley.com/doi/10.1029/2023EF004120 by University Of California, Wiley Online Library on [14/07/2024]. See the Terms

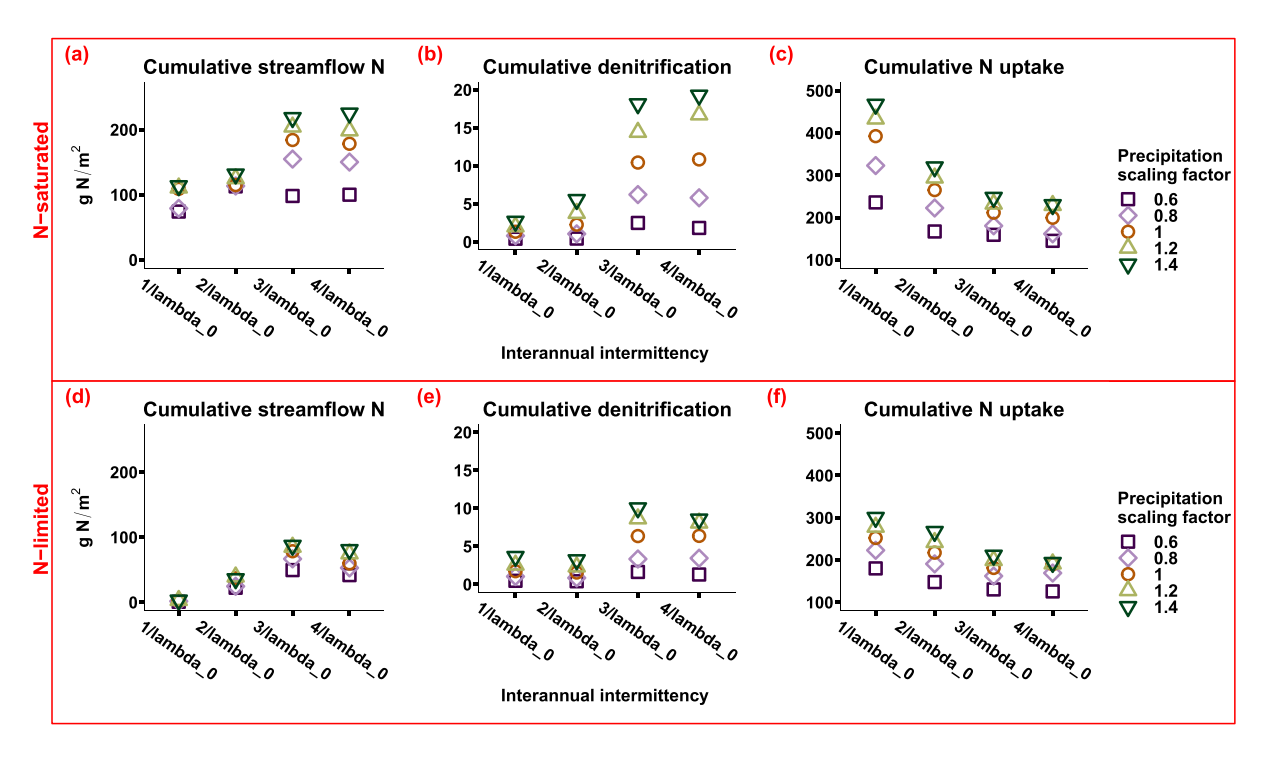


Figure 6. Sensitivity of cumulative N fluxes over 60 years (absolute value) to interannual precipitation intermittency for N-saturated and N-limited scenarios. The *x*-axis is the duration of dry days between rainfall events. Interannual intermittency increases from left to right.

distinct responses to interannual intermittency. First, when the intermittency exceeded $2/\lambda_0$, there was a significant increase in denitrification, which occurred because higher interannual intermittency corresponded with more precipitation per rainfall event, resulting in higher soil moisture levels across the landscape and triggering denitrification in non-hotspot patches (Figures 6b and 6e). However, denitrification started decreasing once interannual intermittency was larger than $3/\lambda_0$. At the highest interannual intermittency levels, increasing the duration of dry months decreased denitrification to a greater extent than larger storms increased it. Plant uptake generally decreased with higher levels of interannual intermittency, which occurred because long-term drought slowed plant growth (Figure S5b in Supporting Information S1). It is worth noting that the magnitude of streamflow nitrate and denitrification in interannual intermittency scenarios is much larger than that of the scenarios for intra-annual intermittency (Figures 4 and 6).

Denitrification and plant N uptake were slightly more sensitive to interannual intermittency in N-saturated scenarios than in N-limited scenarios (Figure 7). This occurred because changes in denitrification and plant growth were constrained by N availability in N-limited scenarios and therefore less responsive to precipitation changes. Streamflow nitrate export was more sensitive to interannual intermittency in N-limited scenarios compared to N-saturated scenarios (Figures 7a and 7d). In N-limited scenarios, drier scenarios showed greater changes to interannual intermittency than wetter scenarios, while in N-saturated scenarios wetter scenarios showed greater changes. This occurred because in N-limited scenarios, drier scenarios had less denitrification and plant uptake, resulting in more nitrate available to be flushed to the stream. It is worth noting that in the N-limited scenario, interannual precipitation intermittency caused the largest changes in streamflow N export compared to intra-annual intermittency and interannual variability.

3.2.3. The Effect of Interannual Precipitation Variability on N Export

In general, scenarios with higher precipitation variance and wetter scaling factors resulted in more streamflow nitrate export (Figure 8). However, for wetter future scenarios, a precipitation scaling factor of 1.2 (rather than 1.4) resulted in the highest streamflow nitrate export (Figures 8a and 8d). This suggests there is a threshold of precipitation increase above which higher flushing capacity is compensated by less available N for flushing with higher denitrification and plant uptake. This can occur because more precipitation can cause higher denitrification and plant N uptake, which can reduce the amount of N available for flushing. Moreover, denitrification rates

REN ET AL. 11 of 21

23284277, 2024, 4, Downloaded from https://agupubs.onlinelibrary.wiley.com/doi/10.1029/2023EF004120 by University Of California, Wiley Online Library on [1407/2024]. See the Terms and Conditions (https://onlinelibrary.wiley.com/term

and-conditions) on Wiley Online Library for rules of use; OA articles are governed by the applicable Creativ

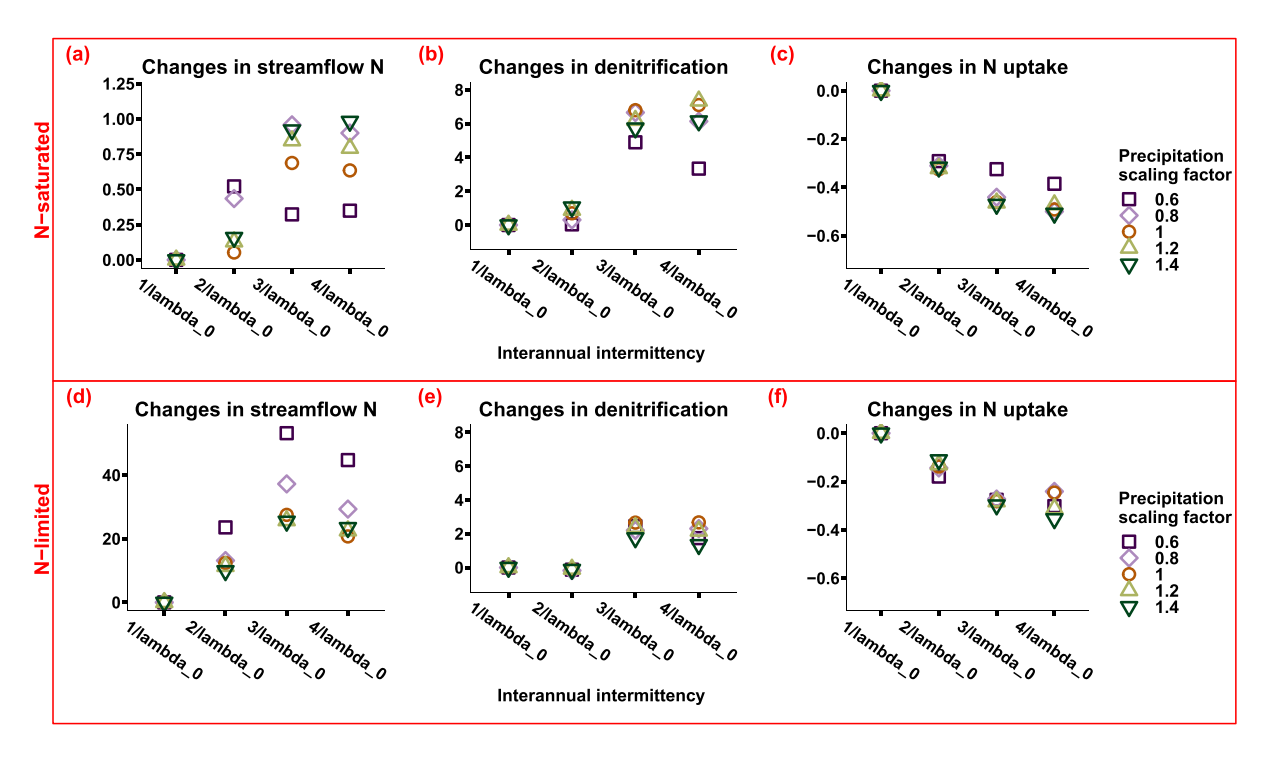


Figure 7. Sensitivity of cumulative N fluxes over 60 years to interannual precipitation intermittency for N-saturated and N-limited scenarios (differences are relative to baseline intermittency; $1/\lambda_{-}0$). The *x*-axis is intermittency, the *y*-axis is normalized change of other intermittencies relative to their baseline intermittency scenarios ($1/\lambda_{-}0$) for every precipitation scaling factor. The top panels are N limited and the bottom panels are N saturated scenarios. Note that the scale of *y*-axis for changes in streamflow N is different for N-saturated and N-limited scenarios.

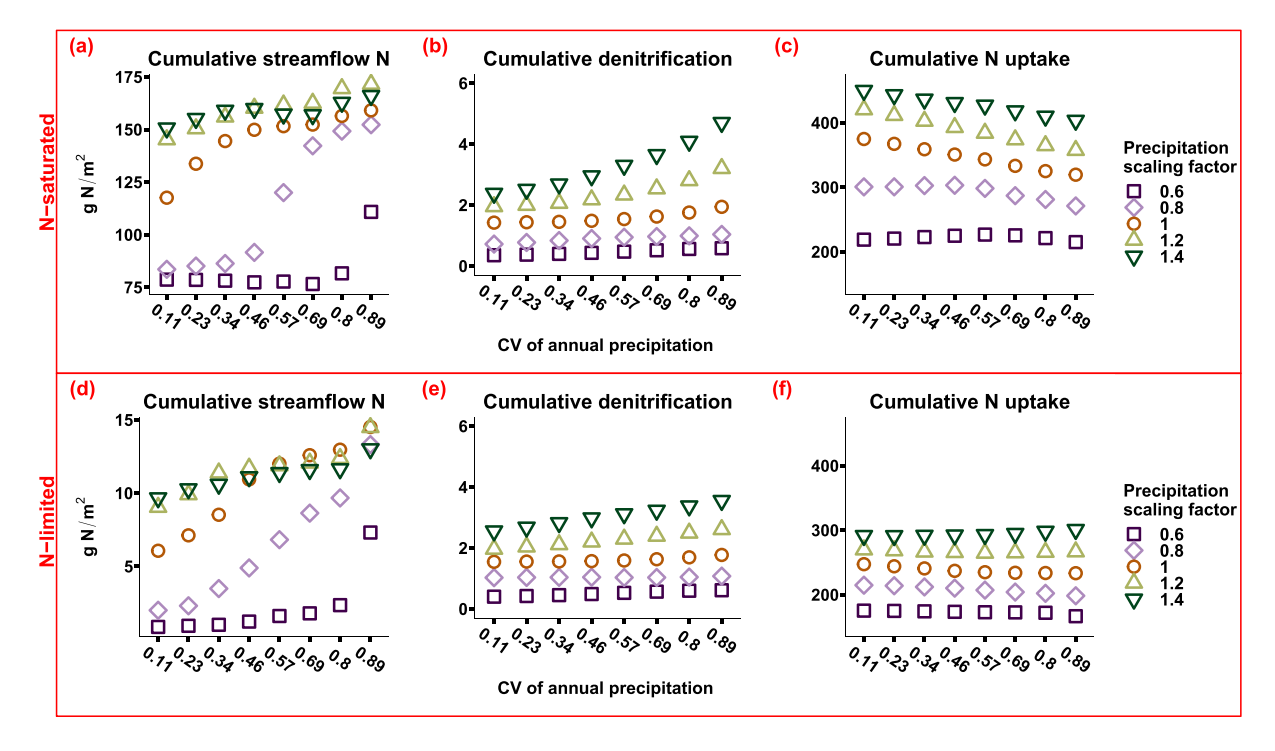


Figure 8. Cumulative N fluxes over 60 years (absolute value) relative to interannual precipitation variability and scaling factors for N-limited and N-saturated scenarios. The *x* axis is the coefficient of variation for annual precipitation, the *y* axis is the cumulative N fluxes over 60 years.

REN ET AL. 12 of 21

23284277, 2024, 4, Downloaded from https://agupubs.onlinelibrary.wiley.com/doi/10.1029/2023EF004120 by University Of California, Wiley Online Library on [14/07/2024]. See the Terms

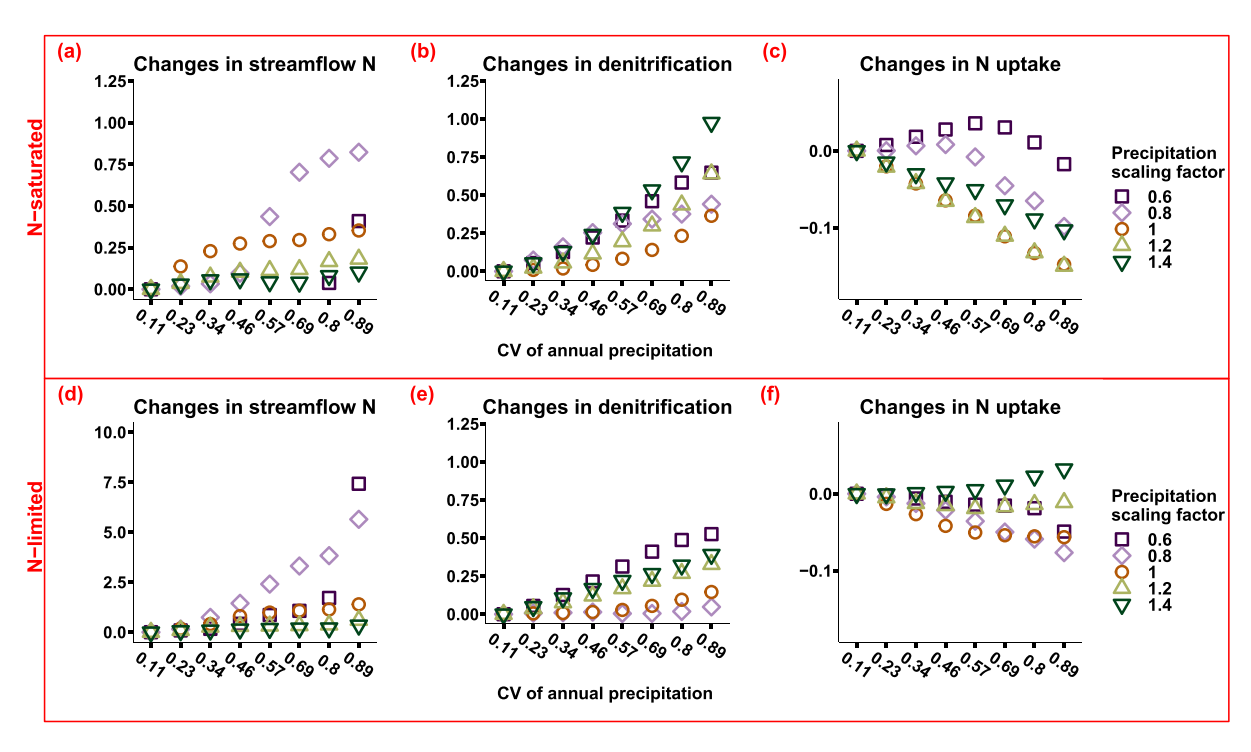


Figure 9. Sensitivity of cumulative N fluxes over 60 years to interannual precipitation variability for N-saturated and N-limited scenarios (differences are relative to the baseline variability scenario which is 0.11). The *x* axis is the coefficient of variation for annual precipitation. The *y* axis is the normalized change in other variances relative to the baseline variability scenario (CV is 0.11) for every precipitation scaling factor (different precipitation scaling factor scenarios have different 0.1 variance baseline scenarios). The top panels are N-saturated and the bottom panels are N-limited scenarios.

increased with higher precipitation variance and a higher precipitation scaling factor (Figures 8b and 8e). Notably, both streamflow nitrate export and denitrification rates were higher in N-saturated compared to N-limited scenarios, due to greater nitrate inputs in N-saturated scenarios.

The sensitivity of N fluxes to precipitation variability differed between N-limited and N-saturated scenarios and was also affected by the precipitation scaling factors (i.e., drier vs. wetter futures; Figure 9). Streamflow N export was more sensitive to precipitation variability in N-limited than in N-saturated scenarios, particularly for the drier future scenarios (Figures 9a and 9d), while denitrification showed the opposite trend (Figures 9b and 9e). The magnitude of sensitivity for plant N uptake was similar between N-limited and N-saturated scenarios, but the direction of effects (i.e., increases or decreases) differed and was affected by the precipitation scaling factor. In the N-limited scenarios, plant N uptake decreased with precipitation variability in drier future scenarios but increased in wetter future scenarios, suggesting that higher precipitation variability can increase plant growth when there is more water available, even if the watershed is N-limited. On the other hand, higher precipitation variability and water stress will suppress plant growth. In N-saturated scenarios, plant N uptake generally decreased with higher precipitation variability, except in some drier scenarios with smaller variability. This suggests that in N-saturated watersheds, less precipitation combined with moderately higher variability can promote plant growth to some extent.

4. Discussion

We investigated how N saturation status, precipitation intermittency, variability, and the total amount of precipitation can interact to influence N export in a dryland watershed in California. We found that streamflow N was more sensitive to intensification of the precipitation regime in N-limited than N-saturated scenarios, whereas the opposite was true for denitrification. Furthermore, changes in interannual precipitation intermittency had the largest effect on streamflow N and denitrification, suggesting that N export may become an even greater threat to water quality when prolonged drought is followed by more intense storm events.

REN ET AL. 13 of 21

4.1. Identifying N Deposition Thresholds for Capacity Saturation

To distinguish between kinetic (i.e., seasonal) and capacity (i.e., long-term) N saturation (Lovett & Goodale, 2011), we developed a simulation modeling approach that quantifies watershed responses to N deposition under different rainfall seasonality regimes. By identifying the amount of N deposition required for precipitation regimes to no longer modify N export, we can approximate when N deposition has exceeded the capacity for plants and microbes to take it up. This approach assumes that kinetic N saturation is more sensitive to precipitation seasonality and timing, which affects plant and microbial N assimilation, while capacity N saturation is less sensitive.

We found that the Bell 4 watershed can become capacity saturated when N deposition reaches 2 g m⁻² year⁻¹ over about 40 years (Figure 3 and Figure S6 in Supporting Information S1). This suggests that the watershed—which has a current mean N deposition rate greater than 2 g m⁻² year⁻¹—has already approached capacity saturation. It is important to note that the threshold we identified is location-specific and is likely to vary with the size, vegetation cover, and climate of a given watershed (Dijkstra et al., 2004; Yu et al., 2018). On average, N deposition is around 0.7 g m⁻² year⁻¹ in dryland watersheds globally and rates are expected to double by 2050 (Benish et al., 2022; Galloway et al., 2008; Kanakidou et al., 2016). Given these increases, many other dryland watersheds could begin to exceed the N deposition thresholds required to shift from a kinetic to capacity saturation in the coming decades. These shifts can pose a major threat to water quality, aquatic ecosystems, and human health. This may be further exacerbated in basins subject to additional sources of N pollution, such as agricultural runoff, sewage discharge, or aquaculture. In such basins, the timing and composition of N loading may differ, and should also be considered when developing N pollution scenarios. Our study provides a useful modeling approach that can be applied to other watersheds to determine N deposition thresholds for establishing capacity N saturation.

4.2. Does an Increase in N Deposition Lead to Greater N Export or N Uptake?

It is essential to distinguish between N-saturated and N-limited watersheds to unravel how changes in the total amount of precipitation and its intermittency or variability will influence watershed processes (Rudgers et al., 2023). In our model setup, N deposition was 100 times higher in N-saturated (5 g m⁻² year⁻¹) than in N-limited scenarios (0.05 g m⁻² year⁻¹). However, the N-saturated/N-limited ratios for various N fluxes (i.e., streamflow nitrate, denitrification, N uptake) were all smaller than 100 (the N deposition rate between N-saturated and N-limited scenarios) and varied among scenarios (Figure S7 in Supporting Information S1). This suggests that N partitioning and soil N storage also changed in response to N-deposition. Not surprisingly, streamflow nitrate had the highest N-saturated/N-limited ratios, ranging from 15 to 80. Denitrification and N uptake, on the other hand, only experienced modest 1-2-fold increases in response to N saturation (Figure S7 in Supporting Information S1). Because most atmospherically deposited N is exported to streams, projected decreases in streamflow (Ficklin et al., 2022; Stephens et al., 2020) could lead to even higher streamflow nitrate concentrations, particularly under increased interannual precipitation variability (Gallo et al., 2015; Ye & Grimm, 2013).

As precipitation regimes become more intermittent and/or variable, N-limited watersheds can retain less N in soil (Winter et al., 2023). In N-limited scenarios, total N export was 25 times higher than the rate of atmospheric N deposition over the 60-year simulation period. This occurred in large part due to declines in plant productivity and N uptake. In N-saturated scenarios, on the other hand, the ratio between N inputs and outputs was consistently less than one, with approximately 20%–60% of the atmospheric N deposition being exported over the 60-year simulation period (Figure 10). The highest N export transfer efficiencies (calculated as the ratio between total N export and N deposition) occurred with high interannual intermittency, while high intra-annual intermittency produced the lowest. Additionally, transfer efficiency can become even higher in a wetter future due to increases in streamflow. Thus, in N-limited scenarios (particularly in a wetter future), increases in precipitation interannual intermittency can increase N export efficiency, thereby reducing N retention capacity in soil. However, our result should be interpreted with care since 25 times higher N transfer efficiency will eventually deplete the N in soil. Conversely, in N-saturated scenarios, a drier future will have lower transfer efficiencies, which can intensify N saturation. This is corroborated by a recent global meta-analysis, which found that reduced precipitation can increase soil N storage over long-term studies, particularly precipitation decreases by more than 25% (Wu et al., 2022).

REN ET AL. 14 of 21

23284277, 2024, 4, Downloaded from https://agupubs.onlinelibrary.wiley.com/doi/10.1029/2023EF004120 by University Of California, Wiley Online Library on [14/07/2024]. See the Terms

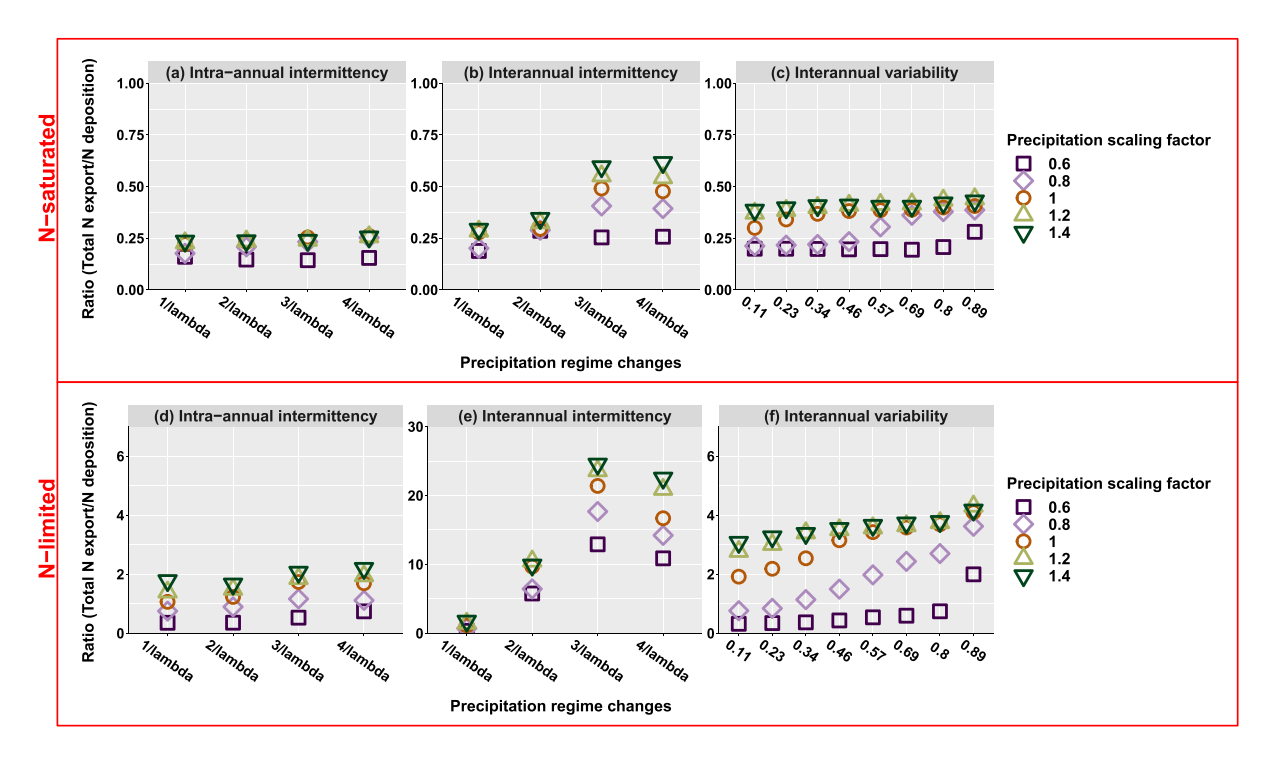


Figure 10. The ratio of total N export (streamflow N and denitrification) to N deposition and its response to precipitation regime changes. For N-saturated scenarios, the N deposition rate was 5 g m⁻² year⁻¹, for N-limited scenarios, it was 0.05 g m⁻² year⁻¹. Ratios larger than 1 indicate N outputs are larger than N inputs and vice versa.

4.3. The Role of Changing Precipitation Regimes

Recent studies have found that precipitation amount and variability both play an important role in driving ecosystem responses to climate change (Gherardi & Sala, 2015, 2019; Jiang et al., 2019; Rudgers et al., 2023). Here we extend those studies to also examine the role of precipitation intermittency and focus on how it affects streamflow nitrate export. In our experimental setup, we ensured water balance among all scenarios (e.g., scenarios with high vs. low interannual intermittency at a given amount of total precipitation had the same total rainfall over the 60-year simulation period). Thus, longer droughts were followed by more precipitation after the drought. Consequently, interannual intermittency scenarios varied both the timing of storms and their magnitude, whereas interannual precipitation variability scenarios only varied the relative magnitude of storms (e.g., some become larger, and some become smaller with increasing variability; Figure 1c). We found that increases in interannual intermittency produced the largest increases (with the greatest variance) in streamflow nitrate among precipitation regime scenarios (Figure 11a). Conversely, interannual variability had the smallest effect on streamflow nitrate. These findings suggest that prolonged drought followed by larger, more intense storms can have the strongest effect on streamflow nitrate. This occurs because multi-year droughts that occur with greater intermittency can reduce N uptake by plants and enable N to accumulate in soils (Krichels et al., 2022; Winter et al., 2023). Subsequent storms then flush accumulated nitrate to streams before plants can take it up.

Denitrification exhibited the most substantial increases with increasing interannual intermittency, whereas it slightly decreased with increasing intra-annual intermittency (Figure 11b). This pattern arose because denitrification is strongly influenced by soil moisture and therefore the amount of precipitation in storm events (Homyak et al., 2016). Increases in both interannual intermittency and variability had large effects on the size of individual storms, while increases in intra-annual intermittency had relatively smaller effects.

Higher intra-annual and interannual precipitation intermittency and variability can all reduce plant growth and corresponding N uptake, but increases in interannual intermittency, which lead to fewer, more intense storms, exert a stronger influence than changes in variability alone (which only affects the relative size of storms without changing their timing). This may occur because longer dry periods can increase soil N accumulation when plants are not active, and that N is subject to leaching or denitrification when more intense rainfall occurs. These findings have important implications for designing field and laboratory experiments aimed at understanding plant

REN ET AL. 15 of 21

23284277, 2024. 4, Downloaded from https://agupubs.onlinelibrary.wiley.com/doi/10.1029/2023EF004120 by University Of California, Wiley Online Library on [14/07/2024]. See the Terms and Condi

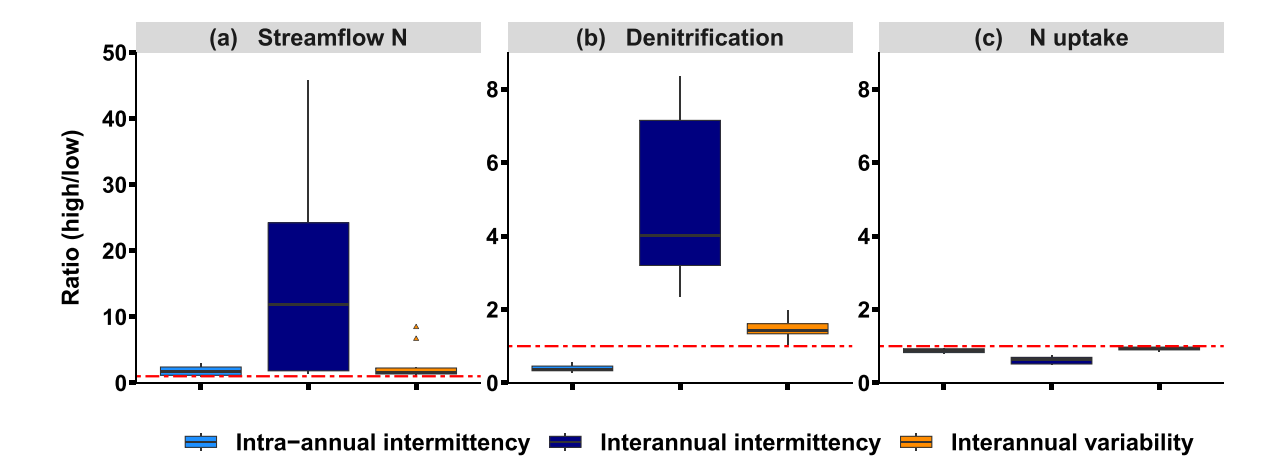


Figure 11. The distribution of ratios of highest intermittency/variability to lowest for different N fluxes. For intermittency this is the ratio between 4/lambda_0 and 1/lambda_0, for variability this is the ratio between 0.89 CV and 0.11 CV. The distribution consists of outputs from all N saturation and precipitation scaling factor scenarios and the variance of distribution indicates how sensitive these N fluxes were to intra-annual intermittency, interannual intermittency, and interannual variability. Note that the *y*-axis for panel (a) is on a different scale than for panels (b and c). The red dashed line represents a ratio of 1, above which N fluxes increase with an intensified precipitation regime and below 1 indicates a decrease.

responses to changing precipitation regimes. Such experiments should not only consider the important roles of storm size and variance (as identified by Gherardi and Sala (2015) and Rudgers et al. (2023)), but should also incorporate intermittency as a key driver.

4.4. Does More Total Precipitation Result in Higher N Export?

Along a gradient from drier to wetter future scenarios, denitrification was the most sensitive flux to increases in total precipitation, followed by streamflow nitrate, while plant N uptake was least affected (Figures 12d-12f). With a 2.3 fold increase of precipitation (from a 0.6 to a 1.4 scaling factor), median denitrification increased approximately 5-7 fold, and this response was slightly greater in N saturated scenarios compared to N-limited scenarios (Figure 12e). This finding aligns with the fact that denitrification is strongly influenced by soil moisture and available nitrate (Poblador et al., 2017). Denitrification is also strongly influenced by soil C (represented as a function of soil respiration in RHESSys), which was higher in wetter future and N-saturated scenarios. Conversely, streamflow nitrate in N-limited scenarios was more responsive to changes in the precipitation scaling factor than in N-saturated scenarios (Figure 12d). In N-limited scenarios, streamflow N increased the precipitation scaling factor, reaching approximately 3.5 times higher than baseline in scenarios with a scaling factor of 1.2. However, it reached an asymptote once the scaling factor exceeded 1.2. This suggests that, for N-limited scenarios, increases in total precipitation do not necessarily translate into higher streamflow nitrate because additional water can enhance denitrification, plant N uptake, and reduce nitrification. Because the effects of total precipitation on streamflow N export are non-linear, it can be challenging to predict N export as precipitation regimes continue to change, particularly in N-limited watersheds (Harms & Grimm, 2008; Homyak et al., 2016).

Changes in the amount of precipitation can also interact with N saturation status to modify various N fluxes. For example, a higher precipitation scaling factor enhanced the N saturation effect on denitrification and its variability (Figure 12h). Alternatively, in drier future scenarios the ratio between N-saturated to N-limited denitrification was smaller than 1 (Figure 12h), suggesting that a drier future can largely inhibit (or even reverse) the N saturation effect, even with 100 times higher N deposition (Wu et al., 2022). With respect to streamflow nitrate, a higher precipitation scaling factor reduced the effects of N saturation and its variability (Figure 12g). This aligns with predictions that a drier future would lead to greater nitrate export to streams and a lower flux to the atmosphere through denitrification (Cregger et al., 2014). Our findings also corroborate recent studies showing that interactions between N deposition and the total amount of precipitation drive N export in drylands (Li et al., 2022).

REN ET AL. 16 of 21

23284277, 2024, 4, Downloaded from https://agupubs.onlinelibrary.wiley.com/doi/10.1029/2023EF004120 by University Of California, Wiley Online Library on [1407/2024]. See the Terms and Conditions (https://onlinelibrary.wiley.com/term/term)

on Wiley Online Library for rules

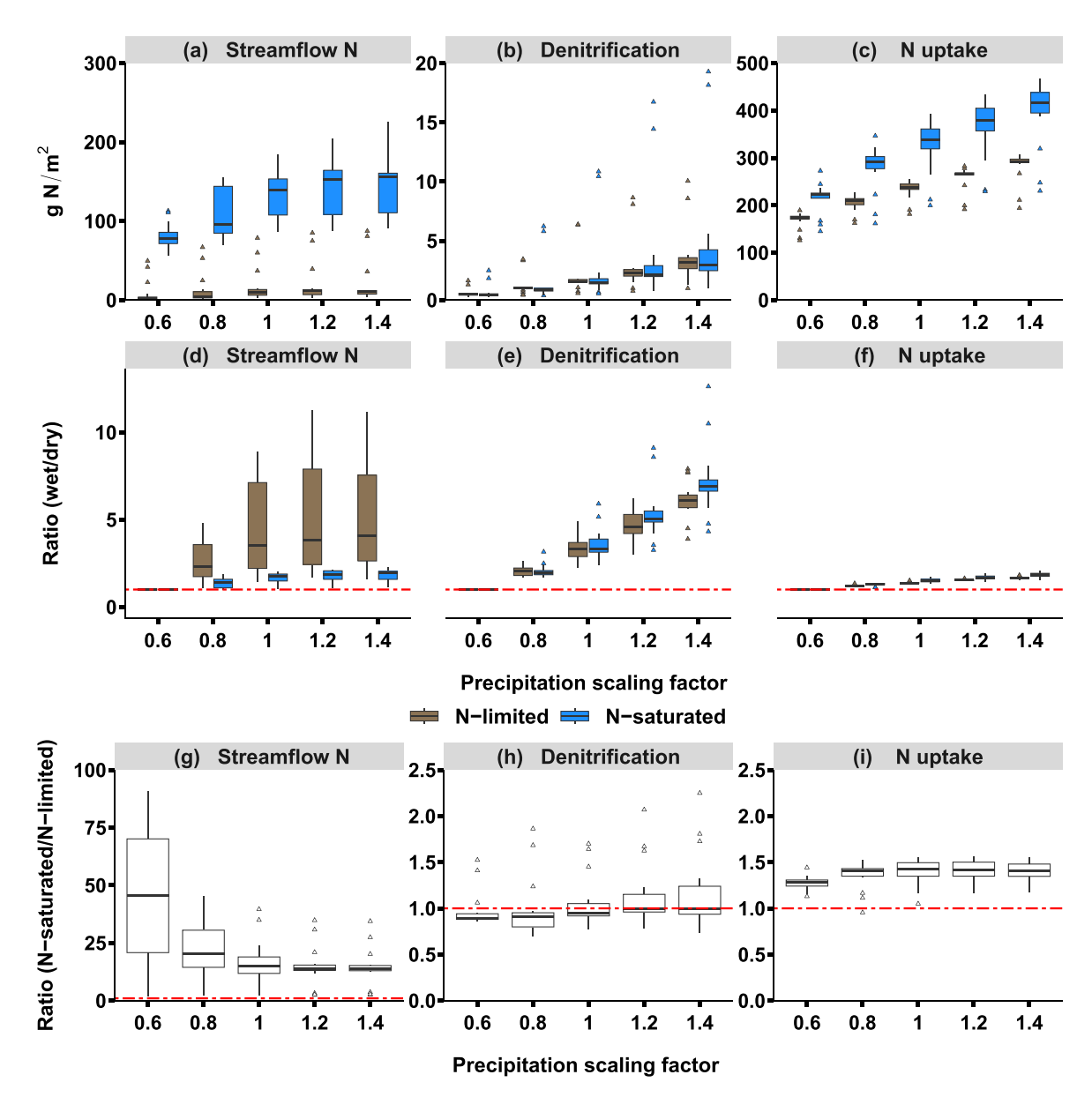


Figure 12. The effect of drier or wetter conditions on N fluxes. The top panels (a–c) represent how cumulative N fluxes over 60 years change with precipitation scaling factor. Each distribution contains both N saturation statuses and all precipitation regime changes. The middle panels of (d–f) represent the ratio of fluxes between precipitation scaling factors larger than 0.6 and the driest scaling factor (i.e., 0.6). The bottom panels g, h and i represent the ratio of fluxes in N-saturated and N-limited conditions and how they vary with the precipitation scaling factor. The dashed blue line denotes a ratio equal to 1.

Although increases or decreases in the total amount of precipitation had smaller effects on N fluxes than increases in intermittency and/or variability, they interacted with precipitation timing to amplify or attenuate their effects. In N-limited scenarios, streamflow N export increased with higher intermittency and variability, but a drier future exaggerated this response whereas a wetter future dampened it (e.g., Figures 5d, 7d, and 9d). Furthermore, even minor decreases in the precipitation scaling factor could substantially increase streamflow nitrate (e.g., Figures 9d and 12g; 0.8 and 0.6 precipitation scaling factors). Thus, the total amount of precipitation can play a critical threshold role in driving how N fluxes respond to increases in precipitation variability and timing (Ficklin et al., 2022).

REN ET AL. 17 of 21

4.5. Study Implications

Predicting future N export in drylands requires considering interaction between hotspots (defined as wetter microsites in the soil that have disproportionately high rates of biogeochemical cycling) and hot moments (defined as wet periods after a prolonged dry spell), rather than treating them as separate entities (Groffman et al., 2009; Kuzyakov & Blagodatskaya, 2015; Pinay et al., 2015). We found that streamflow nitrate and denitrification rates were most sensitive to increases in interannual intermittency. Interannual intermittency scenarios incorporated increases in both the duration of dry periods and the size of storms. In these scenarios, large storms that followed prolonged dry periods can be viewed as hot moments and when these storms surpassed a threshold size (e.g., $2/\lambda_0$ in Figure 7e), denitrification was activated across the basin. Thus, the distribution of "hotspots" can change in response to the timing of hot moments. To better account for the interdependence between hotspots and hot moments, Bernhardt et al. (2017) proposed a new and more comprehensive term: "ecosystem control points." Our research in a dryland chaparral watershed illustrates how ecosystem control points drive N export under a range of future scenarios.

Our modeling framework considered interactions between N saturation status and several ways that precipitation regimes can change. This can serve as a tool for understanding the specific mechanisms driving future N export under climate change. For example, our research highlights the importance of considering the role of interannual intermittency (not just variability) when examining how future precipitation will influence N fluxes. This approach can also help researchers determine the interannual intermittency thresholds that trigger substantial increases in denitrification, which can in turn help them design precipitation manipulation experiments with appropriate intermittency levels.

5. Conclusion

Over the last century, atmospheric N deposition and climate change have increased both greenhouse gas emissions (e.g., NO and N_2O) and stream nitrate export from many dryland watersheds in western North America (Groffman, 2012; Homyak et al., 2016; Krichels et al., 2022). Because these gaseous and hydrologic N fluxes can exacerbate global climate change, decrease aquatic biodiversity, and harm human health (Galloway et al., 2003; Gustine et al., 2022; Meyer et al., 2022), it is important to be able to predict how they will change in the future.

We developed a set of modeling scenarios to examine how N deposition and intensification of the precipitation regime (i.e., the total amount, intermittency, and variability) influence N export in dryland watersheds. To develop these scenarios, we first identified a critical N deposition threshold (~2 g m⁻² year⁻¹) beyond which the watershed shifts from N-limited to N-saturated. Subsequent modeling scenarios revealed that streamflow nitrate export was more sensitive to changes in the timing of precipitation when the watershed was N-limited, whereas denitrification was more sensitive under N-saturation. We also found that drier future scenarios exaggerated the effects of precipitation timing on N export, while there was no uniform response under wetter future scenarios. Notably, among the various ways that precipitation regimes can intensify (i.e., increases in intra-annual intermittency, interannual intermittency, and interannual variability), we found that increases in interannual intermittency caused the largest spikes in N export. High interannual rainfall intermittency enabled solutes like nitrate to build up in hotspots and then be flushed to streams with subsequent intense storms—thus as rainfall intermittency and associated droughts continue to increase, N export will become an increasingly greater threat to water security.

Data Availability Statement

The data sets used to run simulations for this study can be found in Ren et al. (2024b), and the model code is available in Ren et al. (2024c).

References

Abatzoglou, J. T. (2013). Development of gridded surface meteorological data for ecological applications and modelling. *International Journal of Climatology*, 33(1), 121–131. https://doi.org/10.1002/joc.3413

Aber, J. D., Nadelhoffer, K. J., Steudler, P., & Melillo, J. M. (1989). Nitrogen Saturation in Northern Forest Ecosystems: Excess nitrogen from fossil fuel combustion may stress the biosphere. *BioScience*, 39(6), 378–386. https://doi.org/10.2307/1311067

Allen, M. R., & Ingram, W. J. (2002). Constraints on future changes in climate and the hydrologic cycle. *Nature*, 419(6903), 224–232. https://doi.org/10.1038/nature01092

Acknowledgments

This project was supported by the National Science Foundation of the United States under award number DEB-1916658. We thank Tom Dilts for helping with preparing input maps and data for RHESSys. We thank Pete Wohlgemuth for helping with streamflow data processing and model calibration and the USDA Forest Service and the San Dimas Experimental Forest for access to the Bell 4 watershed data. We are grateful to the editor and two anonymous reviewers for their help in improving the quality and clarity of this paper.

REN ET AL. 18 of 21

23284277, 2024, 4, Downloaded from https://agupub

Benish, S. E., Bash, J. O., Foley, K. M., Appel, K. W., Hogrefe, C., Gilliam, R., & Pouliot, G. (2022). Long-term regional trends of nitrogen and sulfur deposition in the United States from 2002 to 2017. Atmospheric Chemistry and Physics, 22(19), 12749–12767. https://doi.org/10.5194/acp-22-12749-2022

Earth's Future

- Bernhardt, E. S., Blaszczak, J. R., Ficken, C. D., Fork, M. L., Kaiser, K. E., & Seybold, E. C. (2017). Control points in ecosystems: Moving beyond the hot spot hot moment concept. *Ecosystems*, 20(4), 665–682. https://doi.org/10.1007/s10021-016-0103-y
- Bettez, N. D., & Groffman, P. M. (2013). Nitrogen deposition in and near an urban ecosystem. *Environmental Science and Technology*, 47(11), 6047–6051. https://doi.org/10.1021/es400664b
- Burke, W. D., Tague, C., Kennedy, M. C., & Moritz, M. A. (2021). Understanding how fuel treatments interact with climate and biophysical setting to affect fire, water, and forest health: A process-based modeling approach. Frontiers in Forests and Global Change, 3. https://doi.org/10.3389/ffgc.2020.591162
- Bytnerowicz, A., & Fenn, M. E. (1996). Nitrogen deposition in California forests: A review. Environmental Pollution, 92(2), 127–146. https://doi.org/10.1016/0269-7491(95)00106-9
- Chaney, N. W., Wood, E. F., McBratney, A. B., Hempel, J. W., Nauman, T. W., Brungard, C. W., & Odgers, N. P. (2016). POLARIS: A 30-meter probabilistic soil series map of the contiguous United States. Geoderma, 274, 54-67. https://doi.org/10.1016/j.geoderma.2016.03.025
- Chen, X., Tague, C. L., Melack, J. M., & Keller, A. A. (2020). Sensitivity of nitrate concentration-discharge patterns to soil nitrate distribution and drainage properties in the vertical dimension. *Hydrological Processes*, 34(11), 2477–2493. https://doi.org/10.1002/hyp.13742
- Cregger, M. A., McDowell, N. G., Pangle, R. E., Pockman, W. T., & Classen, A. T. (2014). The impact of precipitation change on nitrogen cycling in a semi-arid ecosystem. Functional Ecology, 28(6), 1534–1544. https://doi.org/10.1111/1365-2435.12282
- Decina, S. M., Hutyra, L. R., & Templer, P. H. (2020). Hotspots of nitrogen deposition in the world's urban areas: A global data synthesis. Frontiers in Ecology and the Environment, 18(2), 92–100. https://doi.org/10.1002/fee.2143
- Dentener, F., Drevet, J., Lamarque, J. F., Bey, I., Eickhout, B., Fiore, A. M., et al. (2006). Nitrogen and sulfur deposition on regional and global scales: A multimodel evaluation. *Global Biogeochemical Cycles*, 20(4). https://doi.org/10.1029/2005GB002672
- Dickinson, R. E., Shaikh, M., Bryant, R., & Graumlich, L. (1998). Interactive canopies for a climate model. *Journal of Climate*, 11(11), 2823–2836. https://doi.org/10.1175/1520-0442(1998)011<2823;ICFACM>2.0.CO;2
- Dijkstra, F. A., Hobbie, S. E., Knops, J. M. H., & Reich, P. B. (2004). Nitrogen deposition and plant species interact to influence soil carbon
- stabilization. Ecology Letters, 7(12), 1192–1198. https://doi.org/10.1111/j.1461-0248.2004.00679.x

 Du, E. (2016). Rise and fall of nitrogen deposition in the United States. Proceedings of the National Academy of Sciences of the United States of
- America, 113(26), E3594–E3595. https://doi.org/10.1073/pnas.1607543113

 Du, E., de Vries, W., Galloway, J. N., Hu, X., & Fang, J. (2014). Changes in wet nitrogen deposition in the United States between 1985 and 2012.
- Du, E., de Vries, W., Galloway, J. N., Hu, X., & Pang, J. (2014). Changes in wet nitrogen deposition in the United States between 1985 and 2012. Environmental Research Letters, 9(9), 095004. https://doi.org/10.1088/1748-9326/9/9/095004
- Dunn, P. H., Barro, S. C., Wells, W. G., Poth, M. A., Wohlgemuth, P. M., & Colver, C. G. (1988). The San Dimas experimental forest: 50 years of research (No. PSW-GTR-104) (p. PSW-GTR-104). U.S. Department of Agriculture, Forest Service, Pacific Southwest Forest and Range Experiment Station. https://doi.org/10.2737/PSW-GTR-104
- Eagleson, P. S. (1978). Climate, soil, and vegetation: 3. A simplified model of soil moisture movement in the liquid phase. *Water Resources Research*, 14(5), 722–730. https://doi.org/10.1029/WR014i005p00722
- Farquhar, G. D., & von Caemmerer, S. (1982). Modelling of photosynthetic response to environmental conditions. In O. L. Lange, P. S. Nobel, C. B. Osmond, & H. Ziegler (Eds.), *Physiological plant ecology II: Water relations and carbon assimilation* (pp. 549–587). Springer. https://doi.org/10.1007/978-3-642-68150-9 17
- Ficklin, D. L., Null, S. E., Abatzoglou, J. T., Novick, K. A., & Myers, D. T. (2022). Hydrological intensification will increase the complexity of water resource management. *Earth's Future*, 10(3), e2021EF002487. https://doi.org/10.1029/2021EF002487
- Fischer, E. M., Beyerle, U., & Knutti, R. (2013). Robust spatially aggregated projections of climate extremes. *Nature Climate Change*, 3(12), 1033–1038. https://doi.org/10.1038/nclimate2051
- Gallo, E. L., Meixner, T., Aoubid, H., Lohse, K. A., & Brooks, P. D. (2015). Combined impact of catchment size, land cover, and precipitation on streamflow and total dissolved nitrogen: A global comparative analysis. *Global Biogeochemical Cycles*, 29(7), 1109–1121. https://doi.org/10.1002/2015GB005154
- Galloway, J. N., Aber, J. D., Erisman, J. W., Seitzinger, S. P., Howarth, R. W., Cowling, E. B., & Cosby, B. J. (2003). The nitrogen cascade. BioScience, 53(4), 341–356. https://doi.org/10.1641/0006-3568(2003)053[0341:TNC]2.0.CO;2
- Galloway, J. N., Townsend, A. R., Erisman, J. W., Bekunda, M., Cai, Z., Freney, J. R., et al. (2008). Transformation of the nitrogen cycle: Recent trends, questions, and potential solutions. Science, 320(5878), 889–892. https://doi.org/10.1126/science.1136674
- Garcia, E. S., & Tague, C. L. (2015). Subsurface storage capacity influences climate–evapotranspiration interactions in three western United States catchments. Hydrology and Earth System Sciences, 19(12), 4845–4858. https://doi.org/10.5194/hess-19-4845-2015
- Garcia, E. S., Tague, C. L., & Choate, J. S. (2016). Uncertainty in carbon allocation strategy and ecophysiological parameterization influences on carbon and streamflow estimates for two western US forested watersheds. *Ecological Modelling*, 342, 19–33. https://doi.org/10.1016/j.ecolmodel.2016.09.021
- Gherardi, L. A., & Sala, O. E. (2015). Enhanced precipitation variability decreases grass- and increases shrub-productivity. *Proceedings of the National Academy of Sciences of the United States of America*, 112(41), 12735–12740. https://doi.org/10.1073/pnas.1506433112
- Gherardi, L. A., & Sala, O. E. (2019). Effect of interannual precipitation variability on dryland productivity: A global synthesis. *Global Change Biology*, 25(1), 269–276. https://doi.org/10.1111/gcb.14480
- Groffman, P. M. (2012). Terrestrial denitrification: Challenges and opportunities. Ecological Processes, 1(1), 1–11. https://doi.org/10.1186/2192-1709-1-11
- Groffman, P. M., Butterbach-bahl, K., Fulweiler, R. W., Gold, A. J., Morse, J. L., Stander, E. K., et al. (2009). Challenges to incorporating spatially and temporally explicit phenomena (hotspots and hot moments) in denitrification models. *Biogeochemistry*, 93(1–2), 49–77. https://doi.org/10.1007/s10533-008-9277-5
- Gustine, R. N., Hanan, E. J., Robichaud, P. R., & Elliot, W. J. (2022). From burned slopes to streams: How wildfire affects nitrogen cycling and retention in forests and fire-prone watersheds. *Biogeochemistry*, 157(1), 51–68. https://doi.org/10.1007/s10533-021-00861-0
- Hanan, E. J., Ren, J., Tague, C. L., Kolden, C. A., Abatzoglou, J. T., Bart, R. R., et al. (2021). How climate change and fire exclusion drive wildfire regimes at actionable scales. Environmental Research Letters, 16(2), 024051. https://doi.org/10.1088/1748-9326/abd78e
- Hanan, E. J., Tague, C., Choate, J., Liu, M., Kolden, C., & Adam, J. (2018). Accounting for disturbance history in models: Using remote sensing to constrain carbon and nitrogen pool spin-up. Ecological Applications: A Publication of the Ecological Society of America, 28(5), 1197–1214. https://doi.org/10.1002/eap.1718
- Hanan, E. J., Tague, C., & Schimel, J. P. (2017). Nitrogen cycling and export in California chaparral: The role of climate in shaping ecosystem responses to fire. *Ecological Monographs*, 87(1), 76–90. https://doi.org/10.1002/ecm.1234

REN ET AL. 19 of 21

23284277, 2024, 4, Downloaded from https://agupub

1/doi/10.1029/2023EF004120 by University Of California

Wiley Online Library on [14/07/2024]. See

- Harms, T. K., & Grimm, N. B. (2008). Hot spots and hot moments of carbon and nitrogen dynamics in a semiarid riparian zone. *Journal of Geophysical Research*, 113(G1). https://doi.org/10.1029/2007JG000588
- Homyak, P. M., Allison, S. D., Huxman, T. E., Goulden, M. L., & Treseder, K. K. (2017). Effects of drought manipulation on soil nitrogen cycling: A meta-analysis. *Journal of Geophysical Research: Biogeosciences*, 122(12), 3260–3272. https://doi.org/10.1002/2017JG004146
- Homyak, P. M., Blankinship, J. C., Marchus, K., Lucero, D. M., Sickman, J. O., & Schimel, J. P. (2016). Aridity and plant uptake interact to make dryland soils hotspots for nitric oxide (NO) emissions. *Proceedings of the National Academy of Sciences of the United States of America*, 113(19), E2608–E2616. https://doi.org/10.1073/pnas.1520496113
- Homyak, P. M., Sickman, J. O., Miller, A. E., Melack, J. M., Meixner, T., & Schimel, J. P. (2014). Assessing nitrogen-saturation in a seasonally dry chaparral watershed: Limitations of traditional indicators of N-saturation. *Ecosystems*, 17(7), 1286–1305. https://doi.org/10.1007/s10021-014-9792-2
- Howarth, R. W., Swaney, D. P., Boyer, E. W., Marino, R., Jaworski, N., & Goodale, C. (2006). The influence of climate on average nitrogen export from large watersheds in the Northeastern United States. *Biogeochemistry*, 79(1), 163–186. https://doi.org/10.1007/s10533-006-9010-1
- Hubbert, K. R., Preisler, H. K., Wohlgemuth, P. M., Graham, R. C., & Narog, M. G. (2006). Prescribed burning effects on soil physical properties and soil water repellency in a steep chaparral watershed, southern California, USA. *Geoderma*, 130(3), 284–298. https://doi.org/10.1016/j.geoderma.2005.02.001
- Jiang, P., Liu, H., Piao, S., Ciais, P., Wu, X., Yin, Y., & Wang, H. (2019). Enhanced growth after extreme wetness compensates for post-drought carbon loss in dry forests. *Nature Communications*, 10(1), 195. https://doi.org/10.1038/s41467-018-08229-z
- Kanakidou, M., Myriokefalitakis, S., Daskalakis, N., Fanourgakis, G., Nenes, A., Baker, A. R., et al. (2016). Past, present and future atmospheric nitrogen deposition. *Journal of the Atmospheric Sciences*, 73(5), 2039–2047. https://doi.org/10.1175/JAS-D-15-0278.1
- Knapp, A. K., Fay, P. A., Blair, J. M., Collins, S. L., Smith, M. D., Carlisle, J. D., et al. (2002). Rainfall variability, carbon cycling, and plant species diversity in a mesic grassland. Science, 298(5601), 2202–2205. https://doi.org/10.1126/science.1076347
- Knapp, A. K., Hoover, D. L., Wilcox, K. R., Avolio, M. L., Koerner, S. E., La Pierre, K. J., et al. (2015). Characterizing differences in precipitation regimes of extreme wet and dry years: Implications for climate change experiments. *Global Change Biology*, 21(7), 2624–2633. https://doi.org/ 10.1111/gcb.12888
- Krichels, A. H., Greene, A. C., Jenerette, G. D., Spasojevic, M. J., Glassman, S. I., & Homyak, P. M. (2022). Precipitation legacies amplify ecosystem nitrogen losses from nitric oxide emissions in a Pinyon–Juniper dryland. *Ecology*, 104(2), e3930. https://doi.org/10.1002/ecy.3930
 Kuzyakov, Y., & Blagodatskaya, E. (2015). Microbial hotspots and hot moments in soil: Concept & review. *Soil Biology and Biochemistry*, 83,
- Kuzyakov, Y., & Biagodatskaya, E. (2013). Microbial hotspots and hot moments in soil: Concept & review. *Soil Biology and Biochemistry*, & 184–199. https://doi.org/10.1016/j.soilbio.2015.01.025
- Li, Z., Tang, Z., Song, Z., Chen, W., Tian, D., Tang, S., et al. (2022). Variations and controlling factors of soil denitrification rate. *Global Change Biology*, 28(6), 2133–2145. https://doi.org/10.1111/gcb.16066
- Lin, L., Webster, J. R., Hwang, T., & Band, L. E. (2015). Effects of lateral nitrate flux and instream processes on dissolved inorganic nitrogen export in a forested catchment: A model sensitivity analysis. Water Resources Research, 51(4), 2680–2695. https://doi.org/10.1002/2014WR015962
- Lovett, G. M., & Goodale, C. L. (2011). A new conceptual model of nitrogen saturation based on experimental nitrogen addition to an oak forest. *Ecosystems*, 14(4), 615–631. https://doi.org/10.1007/s10021-011-9432-z
- Maxwell, A. E., Warner, T. A., Vanderbilt, B. C., & Ramezan, C. A. (2017). Land cover classification and feature extraction from national agriculture imagery program (NAIP) orthoimagery: A review. *Photogrammetric Engineering and Remote Sensing*, 83(11), 737–747. https://doi.org/10.14358/PERS.83.10.737
- Meyer, M. F., Ozersky, T., Woo, K. H., Shchapov, K., Galloway, A. W. E., Schram, J. B., et al. (2022). Effects of spatially heterogeneous lakeside development on nearshore biotic communities in a large, deep, oligotrophic lake. *Limnology & Oceanography*, 67(12), 2649–2664. https://doi.org/10.1002/lno.12228
- Nash, J. E., & Sutcliffe, J. V. (1970). River flow forecasting through conceptual models part I—A discussion of principles. *Journal of Hydrology*, 10(3), 282–290. https://doi.org/10.1016/0022-1694(70)90255-6
- Parker, S. S., & Schimel, J. P. (2011). Soil nitrogen availability and transformations differ between the summer and the growing season in a California grassland. *Applied Soil Ecology*, 48(2), 185–192. https://doi.org/10.1016/j.apsoil.2011.03.007
- Parton, W. J. (1996). The CENTURY model. In D. S. Powlson, P. Smith, & J. U. Smith (Eds.), Evaluation of soil organic matter models (Vol. 38, pp. 283–291). Springer. https://doi.org/10.1007/978-3-642-61094-3_23
- Phillip, J. (1957). The theory of infiltration: 4. Sorptivity and algebraic infiltration equation. Soil Science, 84, 257–264.
- Pinay, G., Peiffer, S., De Dreuzy, J.-R., Krause, S., Hannah, D. M., Fleckenstein, J. H., et al. (2015). Upscaling nitrogen removal capacity from local hotspots to low stream orders' drainage basins. *Ecosystems*, 18(6), 1101–1120. https://doi.org/10.1007/s10021-015-9878-5
- Poblador, S., Lupon, A., Sabaté, S., & Sabater, F. (2017). Soil water content drives spatiotemporal patterns of CO₂ and N₂O emissions from a Mediterranean riparian forest soil. *Biogeosciences*, 14(18), 4195–4208. https://doi.org/10.5194/bg-14-4195-2017
- H.-O. Pörtner, D. C. Roberts, M. M. B. Tignor, E. S. Poloczanska, K. Mintenbeck, A. Alegría, et al. (Eds.) (2022). Climate change 2022: Impacts, adaptation and vulnerability. In Contribution of Working Group II to the Sixth Assessment Report of the Intergovernmental Panel on Climate Change.
- Ren, J., Hanan, E. J., Abatzoglou, J. T., Kolden, C. A., Tague, C., Kennedy, M. C., et al. (2022). Projecting future fire regimes in a semiarid watershed of the Inland Northwestern United States: Interactions among climate change, vegetation productivity, and fuel dynamics. Earth's Future, 10(3), e2021EF002518. https://doi.org/10.1029/2021EF002518
- Ren, J., Hanan, E. J., Greene, A., Tague, C., Krichels, A. H., Burke, W. D., et al. (2024a). Simulating the role of biogeochemical hotspots in driving nitrogen export from dryland watersheds. *Water Resources Research*, 60(3), e2023WR036008. https://doi.org/10.1029/2023WR036008
- Ren, J., Hanan, E. J., Paolo, D., Tague, C. L., Schimel, J. P., & Homyak, P. M. (2024b). Data for dryland watershed in flux: How nitrogen deposition and changing precipitation regimes shape nitrogen export [Dataset]. *Open Science Forum*. https://doi.org/10.17605/OSF.IO/70TXV
- Ren, J., Hanan, E. J., Paolo, D., Tague, C. L., Schimel, J. P., & Homyak, P. M. (2024c). Code for dryland watershed in flux: How nitrogen deposition and changing precipitation regimes shape nitrogen export (version 7.4) [Software]. Zenodo. https://doi.org/10.5281/zenodo. 7754375
- Reyes, J. J., Tague, C. L., Evans, R. D., & Adam, J. C. (2017). Assessing the impact of parameter uncertainty on modeling grass biomass using a hybrid carbon allocation strategy: A hybrid carbon allocation strategy. *Journal of Advances in Modeling Earth Systems*, 9(8), 2968–2992. https://doi.org/10.1002/2017MS001022
- Rodriguez-Iturbe, I., Porporato, A., Ridolfi, L., Isham, V., & Coxi, D. R. (1999). Probabilistic modelling of water balance at a point: The role of climate, soil and vegetation. *Proceedings of the Royal Society of London. Series A: Mathematical, Physical and Engineering Sciences*, 455(1990), 3789–3805. https://doi.org/10.1098/rspa.1999.0477

REN ET AL. 20 of 21

- Rudgers, J. A., Luketich, A., Bacigalupa, M., Baur, L. E., Collins, S. L., Hall, K. M., et al. (2023). Infrastructure to factorially manipulate the mean and variance of precipitation in the field. *Ecosphere*, 14(7), e4603. https://doi.org/10.1002/ecs2.4603
- Ryan, M. G. (1991a). Effects of climate change on plant respiration. *Ecological Applications*, 1(2), 157–167. https://doi.org/10.2307/1941808 Ryan, T. M. (1991b). In *Soil survey of angeles national forest area* (Vol. 588–137).
- Schimel, J. P. (2018). Life in dry soils: Effects of drought on soil microbial communities and processes. *Annual Review of Ecology Evolution and Systematics*, 49(1), 409–432. https://doi.org/10.1146/annurev-ecolsys-110617-062614
- Stephens, C. M., Marshall, L. A., Johnson, F. M., Ajami, H., Lin, L., & Band, L. E. (2022). Spatial variation in catchment response to climate change depends on lateral moisture transport and nutrient dynamics. *Water Resources Research*, 58(10), e2021WR030577. https://doi.org/10.1029/2021WR030577
- Stephens, C. M., Marshall, L. A., Johnson, F. M., Lin, L., Band, L. E., & Ajami, H. (2020). Is past variability a suitable proxy for future change? A virtual catchment experiment. *Water Resources Research*, 56(2), e2019WR026275. https://doi.org/10.1029/2019WR026275
- Sutton, M. A., Nemitz, E., Erisman, J. W., Beier, C., Bahl, K. B., Cellier, P., et al. (2007). Challenges in quantifying biosphere-atmosphere exchange of nitrogen species. *Environmental Pollution*, 150(1), 125–139. https://doi.org/10.1016/j.envpol.2007.04.014
- Tague, C. L., & Band, L. E. (2004). RHESSys: Regional hydro-ecologic simulation system—An object-oriented approach to spatially distributed modeling of carbon, water, and nutrient cycling. *Earth Interactions*, 8(19), 1–42. https://doi.org/10.1175/1087-3562(2004)8<1:RRHSSO>2.0. CO:2
- Trenberth, K. E., Dai, A., Rasmussen, R. M., & Parsons, D. B. (2003). The changing character of precipitation. *Bulletin of the American Meteorological Society*, 84(9), 1205–1218. https://doi.org/10.1175/BAMS-84-9-1205
- Winter, C., Nguyen, T. V., Musolff, A., Lutz, S. R., Rode, M., Kumar, R., & Fleckenstein, J. H. (2023). Droughts can reduce the nitrogen retention capacity of catchments. *Hydrology and Earth System Sciences*, 27(1), 303–318. https://doi.org/10.5194/hess-27-303-2023
- Wu, Q., Yue, K., Ma, Y., Heděnec, P., Cai, Y., Chen, J., et al. (2022). Contrasting effects of altered precipitation regimes on soil nitrogen cycling at the global scale. *Global Change Biology*, 28(22), 6679–6695. https://doi.org/10.1111/gcb.16392
- Xiao, Q., Hu, Z., Fu, C., Bian, H., Lee, X., Chen, S., & Shang, D. (2019). Surface nitrous oxide concentrations and fluxes from water bodies of the agricultural watershed in Eastern China. *Environmental Pollution*, 251, 185–192. https://doi.org/10.1016/j.envpol.2019.04.076
- Ye, L., & Grimm, N. B. (2013). Modelling potential impacts of climate change on water and nitrate export from a mid-sized, semiarid watershed in the US Southwest. Climatic Change, 120(1), 419–431. https://doi.org/10.1007/s10584-013-0827-z
- Yu, Q., Duan, L., Yu, L., Chen, X., Si, G., Ke, P., et al. (2018). Threshold and multiple indicators for nitrogen saturation in subtropical forests. Environmental Pollution, 241, 664–673. https://doi.org/10.1016/j.envpol.2018.06.001
- Zhu, Q., Castellano, M. J., & Yang, G. (2018). Coupling soil water processes and the nitrogen cycle across spatial scales: Potentials, bottlenecks and solutions. *Earth-Science Reviews*, 187, 248–258. https://doi.org/10.1016/j.earscirev.2018.10.005

REN ET AL. 21 of 21